Bioorganic Chemistry 93 (2019) 103283

Contents lists available at ScienceDirect

Bioorganic Chemistry

journal homepage: www.elsevier.com/locate/bioorg

Design, synthesis and evaluation of some 1,6-disubstituted-*1H*-benzo[*d*] imidazoles derivatives targeted PI3K as anticancer agents

Huai-Wei Ding[a], Lu Yu[b], Meng-xuan Bai[a], Xiao-Chun Qin[b], Man-tong Song[c,*], Qing-Chun Zhao[b,*]

[a] Key Laboratory of Structure-Based Drug Design and Discovery, Ministry of Education, Shenyang Pharmaceutical University, Shenyang 110016, China
[b] School of Traditional Chinese Materia Medica, Shenyang Pharmaceutical University, Shenyang 110016, China
[c] School of Public Health, Shenyang Medical College, Shenyang 110034, China

ARTICLE INFO

Keywords:
Benzo[*d*]imidazole
Antitumor
PI3K

ABSTRACT

Phosphatidylinositol 3-kinase (PI3K) pathway regulates various cellular processes, such as proliferation, growth, autophagy and apoptosis. Class I PI3K is frequently mutated and overexpressed in a lot of human cancers and PI3K was considered as a target for therapeutic treatment of cancer. In this study, we designed and synthesized a series of 1,6-disubstituted-*1H*-benzo[*d*]imidazoles derivatives and evaluated their anticancer activity and the compound **8i** was identified as a lead compound. Compound **8i** with the most potent antiproliferative activity was selected for further biological mechanism. The PI3K kinase assay have shown potent efficiency against four subtypes of PI3K with an IC_{50} of 0.5–1.9 nM. Molecular docking showed a possible formation of H-bonding with essential amino acid residues. Meanwhile, western blot assay indicated that **8i** inhibited cell proliferation via suppression of PI3K kinase activity and subsequently blocked PI3K/Akt pathway activation in HCT116 cells. In addition, **8i** could inhibit the migration and invasion ability of HCT116 cells and could induce apoptosis of HCT116 cells.

1. Introduction

As a member of lipid kinases, the phosphatidylinositol 3-kinase (PI3K) are divided into four different classes: Class I, Class II, Class III and Class IV. The class I PI3K, the most commonly studied, can be further divided into PI3Kα, PI3Kβ, PI3Kδ and PI3Kγ [1–3]. Much evidence indicate that the PI3K pathway plays a key role in various cellular processes, such as proliferation, growth, cell cycle and apoptosis [4,5]. Up to now, lots of PI3K inhibitors had been developed and evaluated in preclinical studies and early clinical trials [6]. Among them, there were four PI3K inhibitors as antineoplastic drugs approved by the FDA (Fig. 1), Idelalisib approved in 2014 [7], Copanlisib approved in 2017 [8], Duvelisib approved in 2018 [9] and Alpelisib approved in 2019 [10].

The design strategy for the target compounds in this work was inspired by GSK2292767 [11] and HS-173 [12–14] (Fig. 2) which are PI3K inhibitors. From the structure of these two compounds, it was found that they had similar molecular characteristics as effective PI3K inhibitors. They contain six-membered rings and five-membered heterocycles, and pyridyl group at position-5. The difference is that GSK2292767 has a substituent at position-4 and HS-173 has a substituent at position-3. According to the mentioned above literature of compound HS-173 and our previous work [15], it suggested that the substituent group should be at position-3 with better activity compare to at position-4. From the perspective of economics of synthesis, it was found that benzoimidazole group could effectively combine the GSK2292767 and HS-173. Not only that, the more active groups of the group R_2 are methyl and 2,4 difluorophenyl base on the conclusion of structure-activity relationships (SARs) in literatures [16–19]. For this reason, our design strategies are concentrated on these two R_2 substituent groups and focusing on the effect of different R_1 on the activity. Interestingly, due to the IUPAC naming rules, the substituent at position-3 of GSK2292767 becomes the position-1 of our target compounds at last by the replacing of pyrazole ring with an imidazole ring base on GSK2292767. Finally, we designed a series of derivatives with benzoimidazoles as the mother nucleus and had different substituents at 1 and 6 positions.

As a result, with the goal of developing some new PI3K inhibitors which might serve as potential drugs for the treatment of cancer, we synthesized a series of compounds containing hydrophilic group at position-1 in benzo[*d*]imidazole. They were prepared and the antitumor effects were investigated *in vitro*. The final results indicate that these series of compounds are a class of pan-PI3K inhibitors and neither like the GSK2292767 as a selective PI3Kγ inhibitor nor like HS-173 as a

* Corresponding authors.
E-mail addresses: songmtong@163.com (M.-t. Song), zhaoqingchun1967@163.com (Q.-C. Zhao).

https://doi.org/10.1016/j.bioorg.2019.103283
Received 20 May 2019; Received in revised form 9 September 2019; Accepted 11 September 2019
Available online 14 September 2019

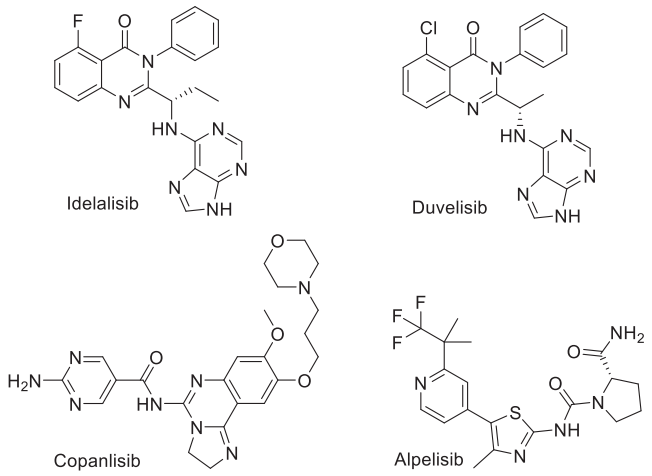

Fig. 1. Four PI3K inhibitors approved by the FDA.

PI3Kα inhibitor. We speculate that the change in the position of the substituent perhaps led to this result. The second perhaps reason is that although HS-173 is reported to be an inhibitor of PI3Kα subtype [13], but the difference in selectivity between four subtypes is not big enough.

2. Results and discussion

2.1. Chemistry

The synthetic routes are showed in Scheme 1. Intermediate **1** was reacted with three amines to yield **2a-c**, which were then be reduced by iron powder in glacial acetic acid and directly added the trimethylorthoformate to afford **3a-c**. **3a-c** were reacted with different halogenated hydrocarbon to abstain **4a-o**, which were then coupled with **7a-b** via Suzuki reaction to afford the target compounds **8a-s**.

2.2. Antiproliferative assays in vitro

All the synthesized compounds were evaluated for their cytotoxicities *in vitro* towards the T47D, MCF-7 and HCT116 cell lines. The results were summarized in Table 1. As shown in Table 1, the cytotoxicities results showed that most of the compounds exhibited potent antiproliferative effects. As the representative, the SARs was discussed with HCT116 cell line. From the overall results, it showed that the activity of hydrophilic groups at position-3 was better than that of hydrophobic groups, including **8b** vs.**8e**, **8d** vs. **8f** and **8i** vs. **8o**. That's why most of the compounds we designed contain alcohol hydroxyl groups. The activity of compounds containing phenyl ring group at position-3 is slightly better than that of compounds containing pyrazoly at the same position, it could be reflected in **8b** vs. **8i**, **8d** vs. **8l** and **8h** vs. **8o**. From the activity of **8i**, **8l** and **8n**, it was possible to draw such a conclusion that the further the hydrophilic group was from the parent nucleus, the lower the activity would be. It also could find that all of compounds with 2,4-difluoro-phenyl group substituent on R_5 position displayed much better antiproliferative activities than those substituted by methyl on the same position, including **8a** vs.**8b**, **8c** vs. **8d**, **8k** vs. **8l** and **8r** vs. **8s**. Introducing methoxy group into benzene ring at R_3 position could not improve the activity, but lead to the decrease of the activity, such as, **8j**, **8m** and **8q**. After the analysis, we hypothesize that introducing methoxy group into the benzene ring will increase hydrophobicity and it is inconsistent with the principle that hydrophilic groups are needed in the ribose pocket.

2.3. *8i* inhibits PI3K and blocks the PI3K-Akt pathway

In order to elucidate the mechanism of antiproliferative activities of these active compounds, we selected the representative compounds **8i** and **8l** for the further PI3K enzymatic activity assays. HS-173 were selected as the positive drugs. As shown in Table 2, kinase inhibition activity assay indicated that the activity of **8i** and **8l** has reached the picomolar level. It found that the kinase activities of **8i** and **8l** were consistent with cellular activities. Two compounds above showed a higher inhibitory activity against PI3Kα when compared to that of other class I PI3Ks (PI3Kβ, PI3Kγ and PI3Kδ).

Docking simulations were conducted to predict the binding model of **8i** in the binding site of PI3K. The structure of PI3K kinase was obtained from protein data bank (PDB entry 3L08, a PI3Kγ isoform [16]). As shown in Fig. 3(A) or (C), the nitrogen of benzo[*d*]imidazole group formed a hydrogen bond with the side chain of Val882 in the hinge binder region of PI3K. Besides, the oxygen of methoxy group formed an additional hydrogen bond interaction with Lys833. Moreover, the nitrogen of pyridyl group formed a hydrogen bond with the conserved water molecule. In addition to these, the hydrogen of hydroxyl group formed a hydrogen bond interaction with Thr887. As shown in Fig. 3(B) and (D), the folded form of compound **8i** in the protein pocket was very similar to that of Omipalisib which was the original ligand in 3L08. Apart from the interaction of hydrogen bonds, the aromatic rings of **8i** also formed Pi-Pi interactions with multiple amino acid residues.

The docking analysis indicated that compound **8i** could fit into the binding site of PI3K kinase, which also indicated that this compound may be a potent PI3K inhibitor.

To further determine whether the PI3K signaling were affected by compound **8i**, Western blot assay was used to evaluate the effects of **8i** on the PI3K related protein levels including Akt and phospho-Akt (p-Akt, S473) in HCT116 cells. As shown in Fig. 4, compared with control group, **8i** experimental group can reduce the protein level of p-Akt in a concentration-dependent manner, indicating that compound **8i** can reduce the activity of p-Akt, and the expression of total protein Akt does not show a change trend. According to the results of Western blot, we can conclude that compound **8i** may inhibit the activity of Akt protein by inhibiting the activation of Akt phosphorylation, thus inhibiting the proliferation of HCT116 cells.

2.4. Colony formation assay of *8i* on HCT116 cells

In order to further investigate the antiproliferation of **8i** on HCT116 cells, the colony formation assay was used to measure the cell viability. As shown in Fig. 5, 8i inhibited the formation of HCT116 cell clones in a concentration-dependent manner, and the high concentration group (3.0 μM) could almost completely inhibit the production of cell clones. The results indicated that HCT116 cells treated with **8i** would lose the ability of cell proliferation.

2.5. Colonic carcinoma cell invasion and migration ability by compound *8i*

The PI3K/Akt signaling pathway plays an important role in cancer cell migration and invasion. To determine the effects of **8i** on colonic carcinoma cell migration and invasion ability, we performed wound healing and invasion assays. For the Transwell invasion assay, **8i** significantly inhibited HCT116 cell metastasis and invasiveness in a dose-dependent manner, after treatment with **8i** for 48 h (Fig. 6A and B).

For wound healing assay, the statistical results (Fig. 6C, D and E) showed that the inhibition ability increased in a concentration-dependent manner.

2.6. Apoptosis induced by compound *8i*

Annexin V-PI double staining assay was used to examine the effect of **8i** on cells apoptosis. As shown in Fig. 7(A and B), compared with the

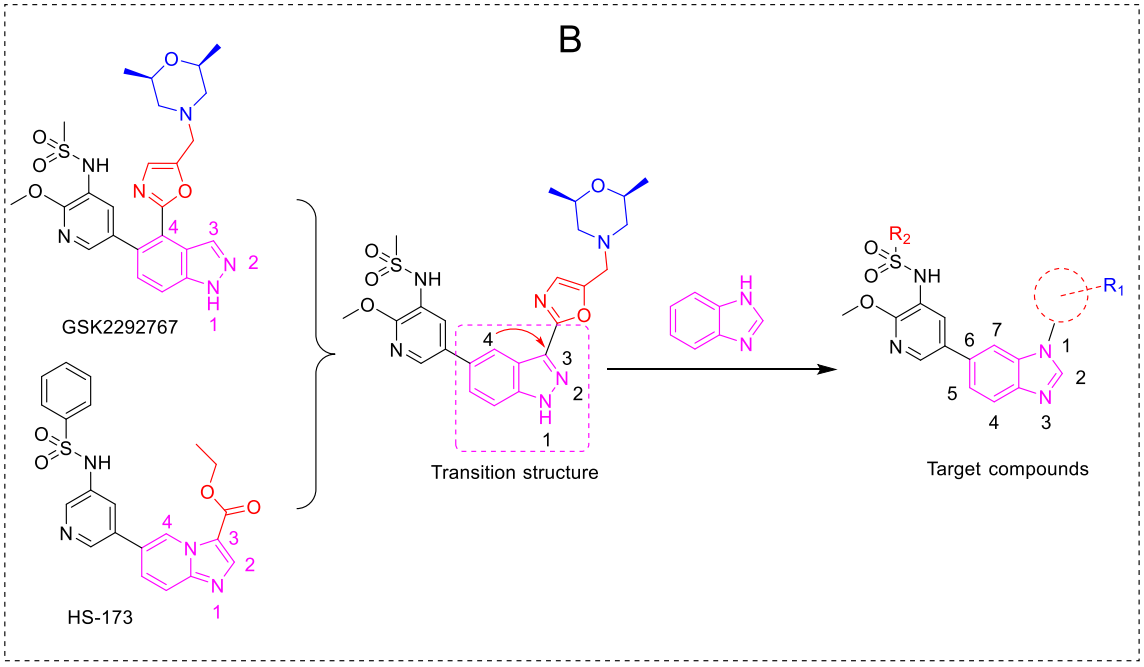

Fig. 2. The design strategy based on GSK2292767 and HS-173.

control group, the proportion of apoptotic cells in compound **8i** treatment group increased significantly and showed a concentration-dependent manner. In summary, the data showed that compound **8i** could induce apoptosis of HCT116 cells. In order to further evaluate **8i**-induced apoptosis in HCT116 cells, cells were stained with Hoechst33342 and analyzed by fluorescence microscope. As shown in Fig. 7(C), treated with different concentrations of **8i**, the brighter fluorescence was seen. Compared with control which had normal

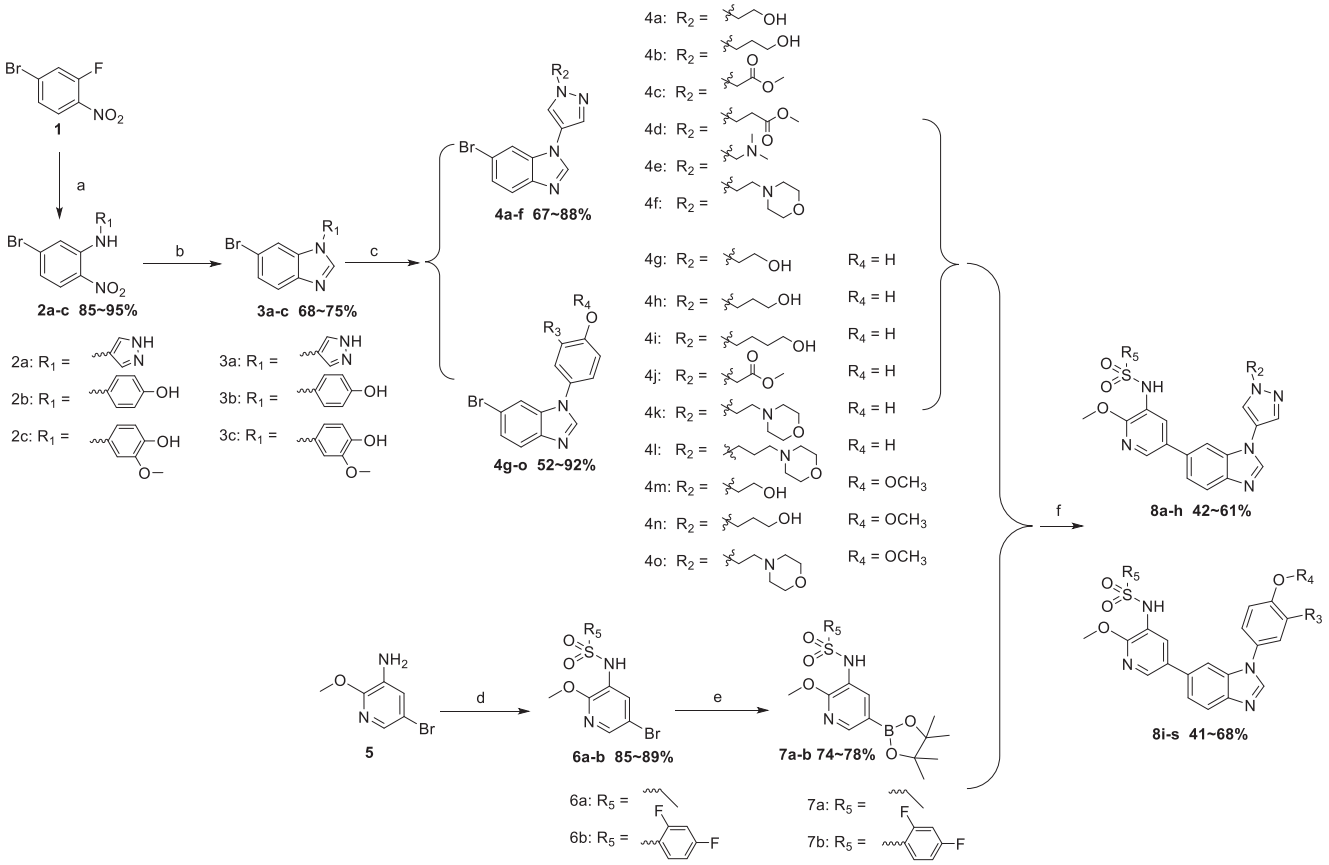

Scheme 1. (a) NH_2-R_1, DMF, DIPEA, 25 °C, 12 h; (b) (1) Fe/CH_3COOH, 90 °C, 6 h; (2) TrimethylOrthoformate, 90 °C, 6 h; (c) Cl-R_2, K_2CO_3, DMF, 60 °C, 12 h; (d) $ClSO_2$-R_5, pyridine, rt, 24 h; (e) bis(pinacolato)diborane, $Pd(dppf)_2Cl_2$, AcOK, DMF, 100 °C, 8 h; (f) Bis(triphenylphosphine)palladium (II) dichloride, Cs_2CO_3, DMF/H_2O, 95 °C, 8 h.

Table 1
Antiproliferative activities of target compounds against three cancer cell lines (IC_{50} Values[a] in μM).

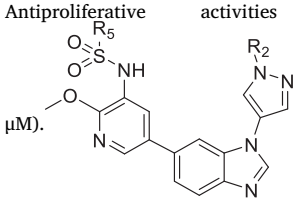

8a-h

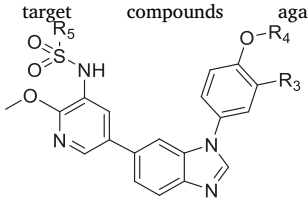

8i-s

Cells Comp.	R_2	R_3	R_4	R_5	T47D	MCF-7	HCT116
8a	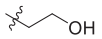	–	–		> 20	9.43 ± 0.14	3.92 ± 0.12
8b	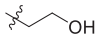	–	–	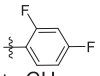	0.27 ± 0.05	0.57 ± 0.09	0.13 ± 0.03
8c	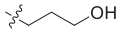	–	–		> 20	16.81 ± 1.12	12.74 ± 0.76
8d	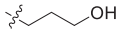	–	–	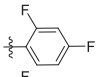	0.29 ± 0.04	0.66 ± 0.09	0.27 ± 0.06
8e	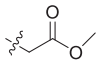	–	–	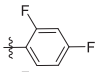	3.26 ± 0.24	4.80 ± 0.18	0.84 ± 0.10
8f	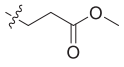	–	–	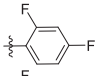	1.14 ± 0.32	0.76 ± 0.14	0.59 ± 0.08
8g	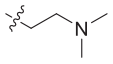	–	–	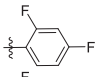	3.58 ± 0.16	1.06 ± 0.12	1.01 ± 0.11
8h	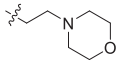	–	–	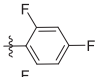	0.67 ± 0.08	0.29 ± 0.04	0.41 ± 0.06
8i	–	H		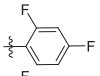	0.36 ± 0.03	0.31 ± 0.02	0.14 ± 0.02
8j	–	OCH_3		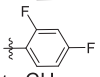	0.62 ± 0.10	0.76 ± 0.02	0.73 ± 0.08
8k	–	H	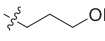		3.99 ± 0.19	1.44 ± 0.12	0.86 ± 0.09
8l	–	H	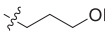	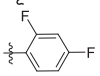	0.45 ± 0.02	0.59 ± 0.03	0.85 ± 0.06
8m	–	OCH_3	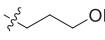	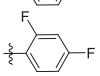	0.75 ± 0.08	1.02 ± 0.12	2.42 ± 0.14
8n	–	H	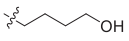	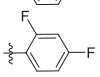	0.89 ± 0.10	0.96 ± 0.12	0.74 ± 0.08
8o	–	H		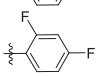	3.92 ± 0.22	4.80 ± 0.34	3.51 ± 0.25
8p	–	H	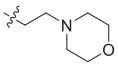	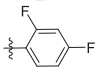	0.54 ± 0.06	0.41 ± 0.02	0.14 ± 0.03
8q	–	OCH_3	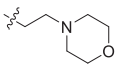	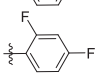	0.68 ± 0.06	0.48 ± 0.02	0.57 ± 0.04
8r	–	H	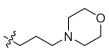		11.22 ± 0.86	4.82 ± 0.32	3.17 ± 0.28
8s	–	H	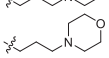		0.29 ± 0.02	0.41 ± 0.03	0.34 ± 0.03
HS-173					0.62 ± 0.12	0.26 ± 0.04	0.54 ± 0.13

[a] IC_{50} values are the mean of triplicate measurements.

Table 2
Enzyme activities of **8i** and **8l** and HS-173 in Class I PI3K (IC_{50} Values in nM).

	PI3Kα	PI3Kβ	PI3Kγ	PI3Kδ
8i	0.50	1.9	1.8	0.74
8l	0.82	5.5	2.9	1.3
HS-173	1.1	59.2	104	87

nuclear morphology after Hoechst33342 staining, **8i** treatment group marked with nuclear fragmentation and condensation of chromatin.

2.7. ADME evaluation

Drug likeliness properties of the compound **8i** was calculated by the help of SwissADME online software. The results are presented in Table 3. According to Lipinski's rule of five, total number of HBD should

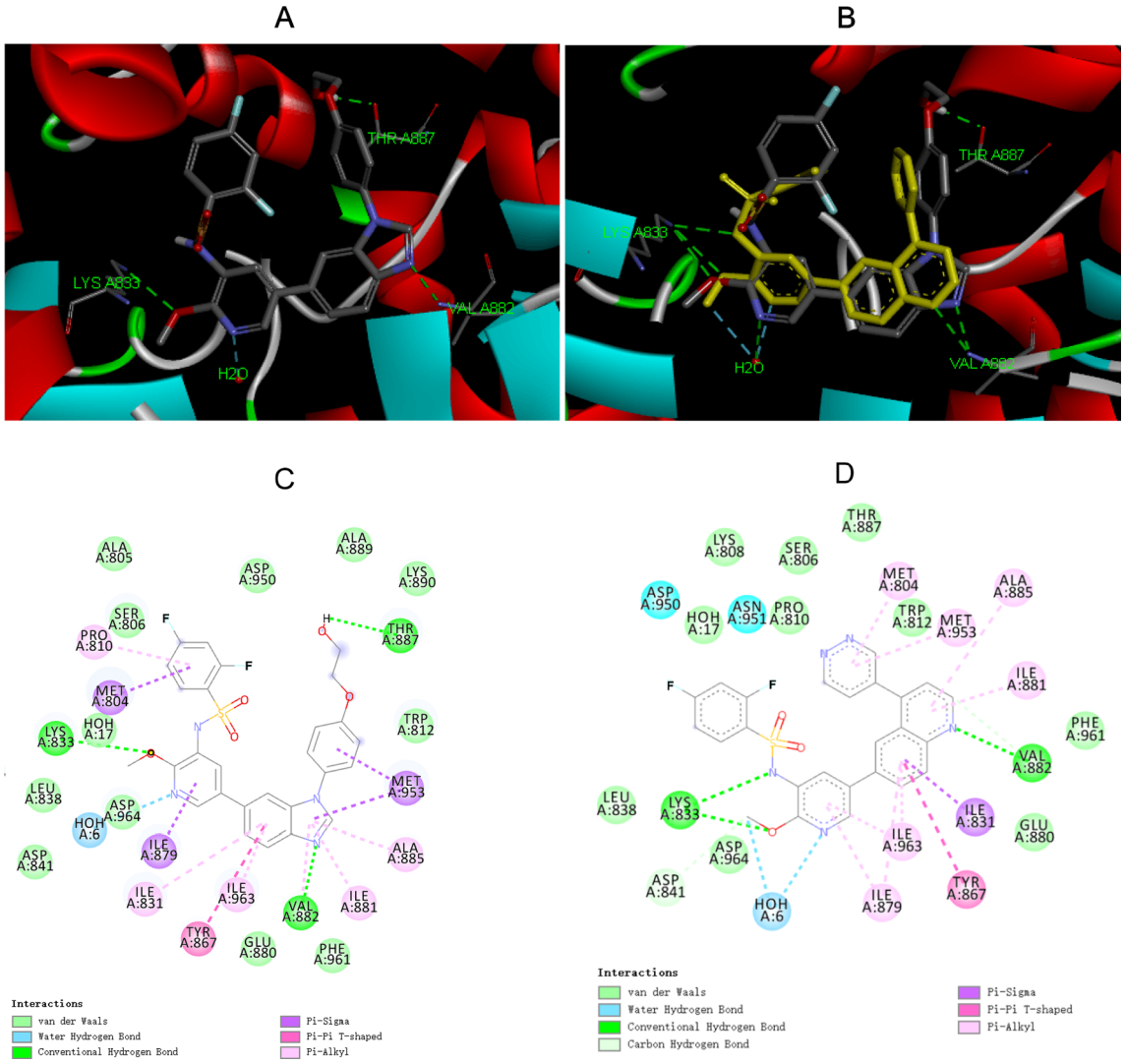

Fig. 3. Docking mode of **8i** with protein crystal structure of PI3K. (A) Key interactions of compound **8i** in the active site of PI3K (PDB: 3L08). (B) The binding pose of **8i** and Omipalisib in the active site of PI3K. Omipalisib was highlighted with yellow. (C) Two-dimensional graph of compound **8i** in the active site of PI3K. (D) Two-dimensional graph of Omipalisib in the active site of PI3K.

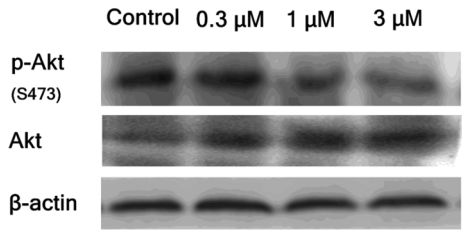

Fig. 4. The inhibition effects of compound **8i** (0.3 μM, 1 μM and 3 μM) on the expression of p-Akt, Akt in HCT116 cells are depicted. β-Actin was used as internal control.

not be more than 5, and total number of HBA should not be greater than 10. Number of HBD and HBA of **8i** are determined 2 and 9 respectively. Topological polar surface area (TPSA, > 140 A^2 is linked with low blood-brain barrier (BBB) penetration, and poor membrane permeability [20]) is a very useful parameter for prediction of transport of drug molecule and the TPSA of **8i** was 123.95 A^2. Estimation of lipophilicity is determined by clogP, which is the log of octanol/water partition coefficient. The clogP value should not be greater than 5. Predicted by software, **8i** has a favourable clogP value (4.10) and it demonstrates that could have good membrane permeability. Unfortunately, **8i** has a molecular weight of 552 which violates the Lipinski's rule of five. However, many anticancer drugs approved by FDA also have a molecular weight greater than 500, such as Quizartinib (MW: 560) and Neratinib (MW: 557), so this may not particularly affect the compound **8i** as a good potential candidate.

3. Conclusion

In summary, some 1,6-disubstituted-1H-benzo[*d*]imidazoles derivatives were designed and synthesized and the antiproliferative activities against three cancer cell lines, including T47D, HCT116 and MCF-7. Compound **8i** with the most potent antiproliferative activity was selected for further biological evaluation. The PI3K kinase assay and western blot assay indicated that **8i** inhibited cell proliferation via blocking the PI3K/Akt pathway in HCT116 cells. In addition, the colony formation assay and apoptosis assay suggested that **8i** could inhibit the migration and invasion ability of HCT116 cells. ADME screening demonstrated that **8i** possessed drug-like properties to become biologically active molecules. According to these results, compound **8i** could be as a potential PI3K inhibitor and could be considered as a potential candidate for anticancer drug development.

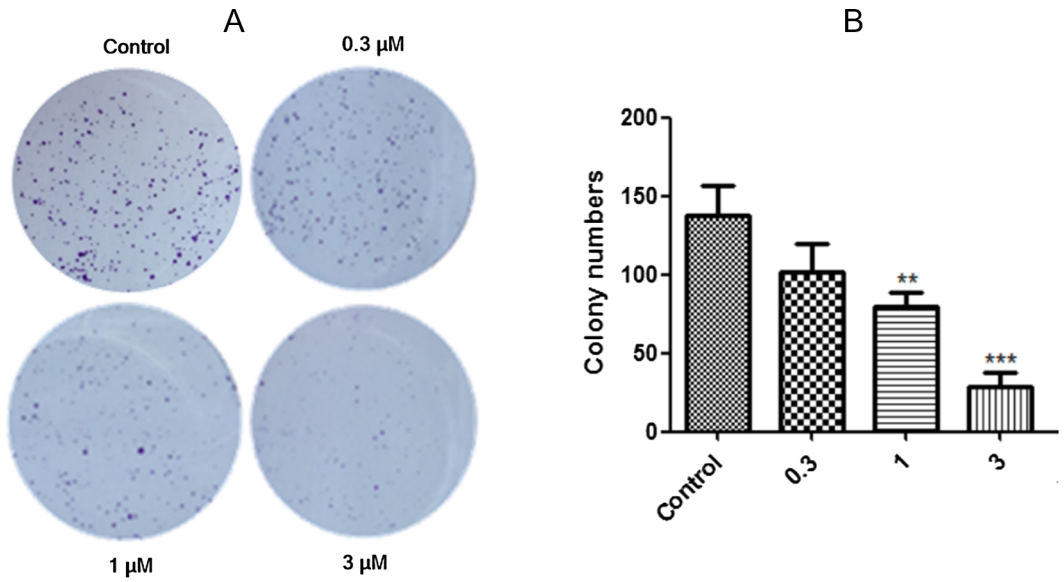

Fig. 5. The colony formation assay of compound **8i**. Treatment with compound **8i**, representative photographs of colony formation are shown. Data are presented as the mean for three independent experiments. **P < 0.01, ***P < 0.001 compared with control.

4. Experimental section

4.1. Chemistry and chemical methods

The reagents and solvents were commercially available without further purification. ^{13}C NMR spectra and ^{1}H NMR spectra were tested on 400 and 600 Bruker NMR spectrometer with tetramethylsilane (TMS) as an internal standard and the chemical shifts are reported in ppm (δ) and coupling constants (J) are in hertz (Hz). The melting points were determined on a Beijing micromelting-point apparatus and thermometer was uncorrected. High-resolution exact mass measurements were performed using electrospray ionization (positive mode) on a quadrupole time-of-flight (QTOF) mass spectrometer (microTOF-Q, Bruker Inc.).

4.1.1. N-(5-Bromo-2-nitrophenyl)-1H-pyrazol-4-amine (2a)

To a solution of 4-bromo-2-fluoro-1-nitrobenzene (**1**, 2.19 g, 10 mmol) in DMF (50 ml) and DIPEA (10 ml) at 25 °C was added 1H-pyrazol-4-amine (1.25 g, 15 mmol). Then the mixture was stirred at room temperature 12 h. DMF and DIPEA were removed at reduced pressure and add water (100 ml), and the residue was purified through a column chromatography on silica with chloroform/methanol (V:V 20:1) as a red solid. (2.68 g, 95.0% yield). mp 94–96 °C.^{1}H NMR (400 MHz, DMSO-d_6) δ 13.03 (s, 1H, NH), 9.19 (s, 1H, NH), 8.03 (d, J = 9.1 Hz, 1H, Ar−H), 7.96–7.58 (m, 2H, Ar−H), 7.06 (d, J = 2.0 Hz, 1H, Ar−H), 6.93 (dd, J = 9.1, 2.0 Hz, 1H, Ar−H). ^{13}C NMR (100 MHz, DMSO-d_6) δ 145.63, 136.48, 131.50, 130.93, 128.51, 125.80, 120.00, 119.94, 118.08. ESI-MS: m/z 281.1 $[M-H]^+$.

Compounds **2b-c** was synthesized according to the procedure described in **2a**.

4.1.2. 4-((5-Bromo-2-nitrophenyl)amino)phenol (2b)

94.4% yield. mp 155–157 °C. ^{1}H NMR (400 MHz, DMSO-d_6) δ 9.66 (s, 1H, OH), 9.42 (s, 1H, NH), 8.03 (d, J = 9.3 Hz, 1H, Ar−H), 7.14 (d, J = 8.6 Hz, 2H, Ar−H), 6.93 (s, 1H, Ar−H), 6.90 (d, J = 2.0 Hz, 1H, Ar−H), 6.86 (d, J = 8.7 Hz, 2H, Ar−H). ^{13}C NMR (100 MHz, DMSO-d_6) δ 156.57, 145.43, 131.49, 130.62, 129.48, 128.61, 128.18 (2C), 119.81, 118.19, 116.75 (2C). ESI-MS: m/z 309.0 $[M+H]^+$.

4.1.3. 4-((5-Bromo-2-nitrophenyl)amino)-2-methoxyphenol (2c)

85.6% yield. mp 138–141 °C. ^{1}H NMR (400 MHz, DMSO-d_6) δ 9.42 (s, 1H, OH), 9.22 (s, 1H, NH), 8.03 (d, J = 9.1 Hz, 1H, Ar−H), 7.01 (d, J = 2.0 Hz, 1H, Ar−H), 6.94 (s, 1H, Ar−H), 6.91 (d, J = 2.0 Hz, 1H, Ar−H), 6.86 (d, J = 8.3 Hz, 1H, Ar−H), 6.76 (dd, J = 8.3, 2.2 Hz, 1H, Ar−H), 3.77 (s, 3H, CH_3). ^{13}C NMR (100 MHz, DMSO-d_6) δ 148.78, 145.78, 145.32, 131.50, 130.63, 129.76, 128.54, 119.91, 118.96, 118.43, 116.31, 111.35, 56.21. ESI-MS: m/z 338.9 $[M+H]^+$.

4.1.4. 6-Bromo-1-(1H-pyrazol-4-yl)-1H-benzo[d]imidazole (3a)

A solution of the **2a** (2.82 g, 10 mmol), iron powder (2.8 g, 50 mmol) in CH_3CH_2COOH (100 ml) was stirred at 90 °C for 6 h. Without purified and directly added the TrimethylOrthoformate (10 ml), then the solution stirred at 90 °C for another 6 h. CH_3CH_2COOH was removed under reduced pressure and add water (100 ml), whereby a white solid precipitate formed. The precipitate was washed with water (20 ml), dried to give compound **3a** as a white solid (1.97 g, 75.2% yield). mp 179–182 °C.^{1}H NMR (400 MHz, DMSO-d_6) δ 13.36 (s, 1H, NH), 8.50 (s, 1H, Ar−H), 8.22 (d, J = 165.2 Hz, 2H, Ar−H), 7.74 (d, J = 1.6 Hz, 1H, Ar−H), 7.71 (d, J = 8.6 Hz, 1H, Ar−H), 7.44 (dd, J = 8.6, 1.7 Hz, 1H, Ar−H). ^{13}C NMR (100 MHz, DMSO-d_6) δ 145.19, 142.81, 135.37, 133.90, 125.76, 123.85, 121.92, 118.49, 116.29, 113.90. ESI-MS: m/z 260.5 $[M+H]^+$.

Compounds **3b-c** were synthesized according to the procedure described in **3a**.

4.1.5. 4-(6-Bromo-1H-benzo[d]imidazol-1-yl)phenol (3b)

72.3% yield. mp 153–155 °C.^{1}H NMR (400 MHz, DMSO-d_6) δ 9.93 (s, 1H, OH), 8.48 (s, 1H, Ar−H), 7.72 (d, J = 8.5 Hz, 1H, Ar−H), 7.62 (s, 1H, Ar−H), 7.48–7.44 (m, 2H, Ar−H), 7.42 (s, 1H, Ar−H), 6.99 (d, J = 8.5 Hz, 2H, Ar−H). ^{13}C NMR (100 MHz, DMSO-d_6) δ 157.86, 145.00, 143.05, 135.44, 127.15, 126.22 (2C), 125.62, 122.02, 116.84 (2C), 116.07, 113.67. ESI-MS: m/z 289.0 $[M+H]^+$.

4.1.6. 4-(6-Bromo-1H-benzo[d]imidazol-1-yl)-2-methoxyphenol (3c)

68.8% yield. mp 202–204 °C. ^{1}H NMR (400 MHz, DMSO-d_6) δ 9.50 (s, 1H, OH), 8.50 (s, 1H, Ar−H), 7.72 (d, J = 8.6 Hz, 1H, Ar−H), 7.68 (d, J = 1.7 Hz, 1H, Ar−H), 7.43 (dd, J = 8.6, 1.8 Hz, 1H, Ar−H), 7.21 (d, J = 2.3 Hz, 1H, Ar−H), 7.04 (dd, J = 8.3, 2.4 Hz, 1H, Ar−H), 6.98 (d, J = 8.4 Hz, 1H, Ar−H), 3.86 (s, 3H, CH_3). ^{13}C NMR (100 MHz, DMSO-d_6) δ 148.83, 147.12, 145.11, 143.01, 135.48, 127.29, 125.64, 121.98, 117.18, 116.29, 116.09, 113.84, 109.66, 56.42.. ESI-MS: m/z 318.7 $[M+H]^+$

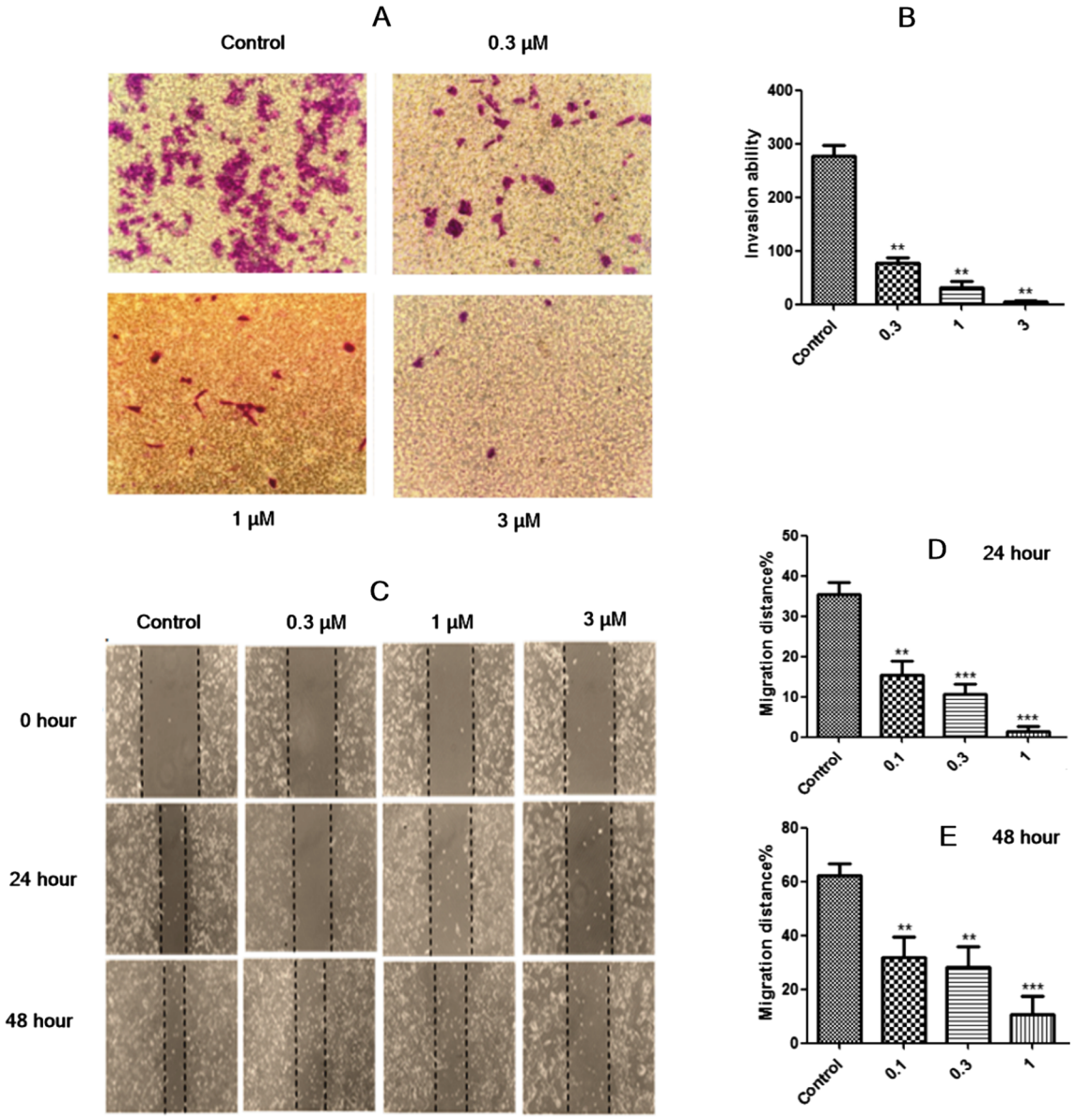

Fig. 6. Transwell invasion and wound healing assays of compound **8i**. (A) Treatment with compound **8i**, representative photographs of invasion are shown. (B) Quantification of the percentages of cells at different concentration. (C) Photographs of wound healing assay. (D) Quantification of the percentages of transfection group (24 h). (E) Quantification of the percentages of transfection group (48 h). Data are presented as the mean for three independent experiments. ** $P < 0.01$, *** $P < 0.001$ compared with control.

*4.1.7. 2-(4-(6-Bromo-1H-benzo[d]imidazol-1-yl)-1H-pyrazol-1-yl)ethan-1-ol (**4a**)*

A solution of the **3a** (0.26 g, 1 mmol) in DMF (20 ml) to add K_2CO_3 (0.28 g, 2 mmol) at 25 °C and this solution was stirred at 25 °C for 10 min. Then added into 1H-pyrazol-4-amine (1.25 g, 15 mmol) and the solution was stirred at 60 °C for 12 h. DMF was removed under reduced pressure and the residue was purified through a column chromatography on silica with chloroform/methanol (V:V 10:1) as a white oil (0.19 g, 60.4% yield).^{1}H NMR (400 MHz, DMSO-d_6) δ 8.56 (s, 1H, Ar−H), 8.45 (s, 1H, Ar−H), 8.02 (s, 1H, Ar−H), 7.83–7.81 (m, 1H, Ar−H), 7.77 (d, J = 8.6 Hz, 1H, Ar−H), 7.51–7.47 (m, 1H, Ar−H), 5.06 (s, 1H, OH), 4.29 (t, J = 5.5 Hz, 2H, CH_2), 3.88 (t, J = 5.5 Hz, 2H, CH_2). ^{13}C NMR (100 MHz, DMSO-d_6) δ 145.04, 142.76, 136.02, 135.31, 128.43, 125.42, 120.50, 116.77, 115.12, 113.23, 60.35, 55.29. ESI-MS: m/z 307.1 $[M+H]^+$.

Compounds **4b-o** were synthesized according to the procedure described in **4a**.

*4.1.8. 3-(4-(6-Bromo-1H-benzo[d]imidazol-1-yl)-1H-pyrazol-1-yl) propan-1-ol (**4b**)*

81.2% yield. Oil.^{1}H NMR (400 MHz, DMSO-d_6) δ 8.51 (s, 1H, Ar−H), 8.44 (s, 1H, Ar−H), 7.98–7.95 (m, 1H, Ar−H), 7.77 (d, J = 1.6 Hz, 1H, Ar−H), 7.71 (d, J = 8.6 Hz, 1H, Ar−H), 7.44 (dd, J = 8.6, 1.8 Hz, 1H, Ar−H), 4.73 (s, 1H, OH), 4.26 (t, J = 7.1 Hz, 2H, CH_2), 3.46 (t, J = 6.1 Hz, 2H, CH_2), 2.01 (p, J = 6.4 Hz, 2H, CH_2). ^{13}C NMR (100 MHz, DMSO-d_6) δ 144.96, 142.77, 135.15, 133.43, 125.82, 125.14, 121.95, 118.39, 116.35, 113.89, 58.15, 49.72, 33.40. ESI-MS: m/z 321.1 $[M+H]^+$.

*4.1.9. Methyl 2-(4-(6-bromo-1H-benzo[d]imidazol-1-yl)-1H-pyrazol-1-yl) acetate (**4c**)*

88.6% yield. mp 96–98 °C.^{1}H NMR (400 MHz, DMSO-d_6) δ 8.56 (s, 1H, Ar−H), 8.48 (s, 1H, Ar−H), 8.05 (s, 1H, Ar−H), 7.74 (s, 1H, Ar−H), 7.72 (d, J = 5.7 Hz, 1H, Ar−H), 7.45 (dd, J = 8.6, 1.8 Hz, 1H, Ar−H), 5.21 (s, 2H, CH_2), 3.74 (s, 3H, CH_3). ^{13}C NMR (100 MHz, DMSO-d_6) δ

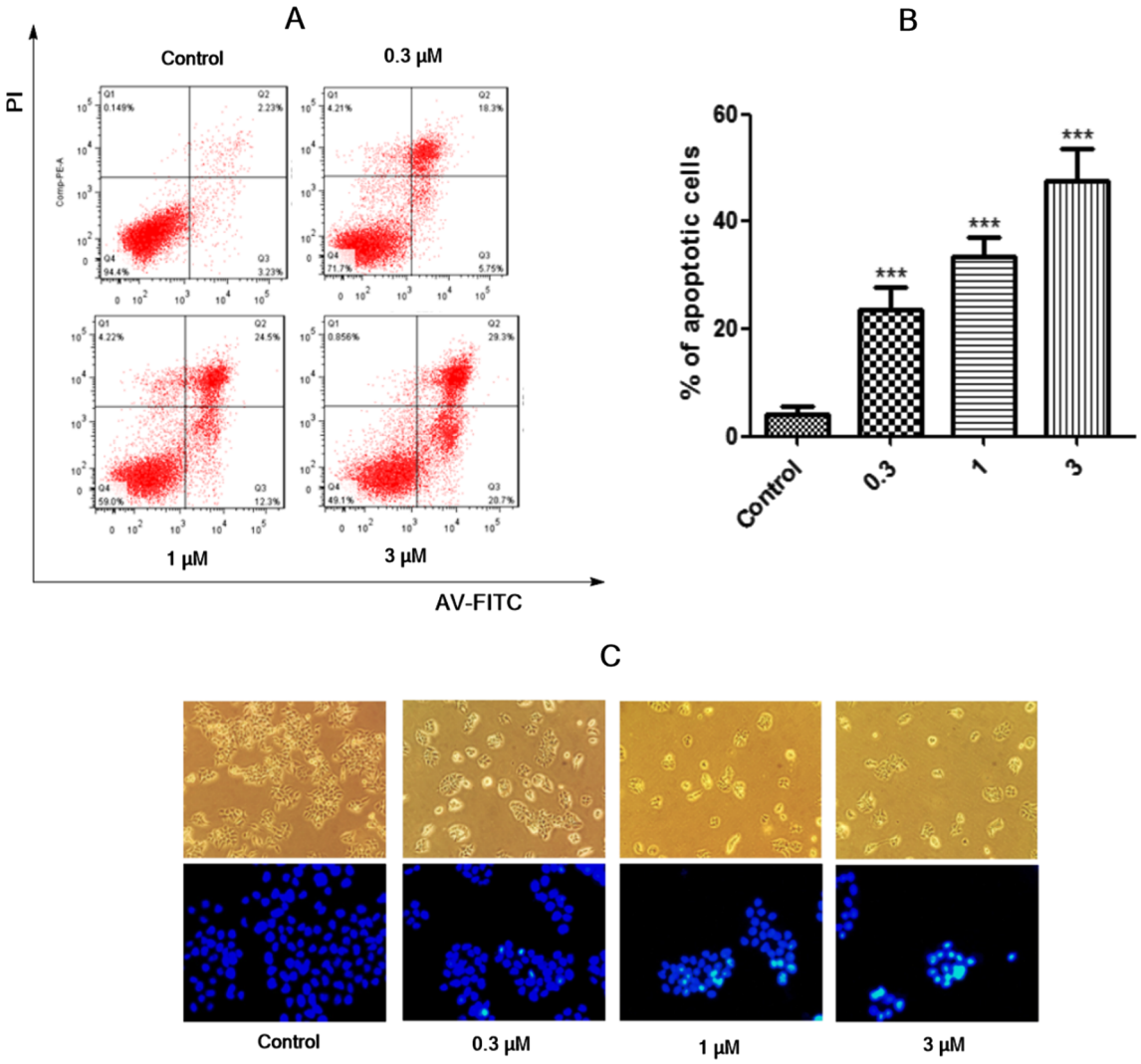

Fig. 7. 8i induced apoptosis in HCT116 cells. (A) AV-PI staining show early and late apoptosis of HCT116 cells induced by compound **8i**. (B) Quantification of early and late apoptosis. (C) The nuclei morphology changes of HCT116 cells treated with **8i** visualized by Hoechst 33342. Data are presented as the mean for three independent experiments. *** $P < 0.001$ compared with control.

168.89, 162.76, 144.87, 142.81, 135.05, 134.30, 126.39, 125.89, 122.06, 119.10, 116.39, 113.74, 53.51, 52.84. ESI-MS: *m/z* 334.9 $[M+H]^+$.

*4.1.10. Methyl 3-(4-(6-bromo-1H-benzo[d]imidazol-1-yl)-1H-pyrazol-1-yl)propanoate **(4d)***

83.4% yield. mp 80–83 °C. ^{1}H NMR (400 MHz, DMSO-d_6) δ 8.51 (s, 1H, Ar—H), 8.45 (s, 1H, Ar—H), 7.98 (s, 1H, Ar—H), 7.76 (d, J = 1.7 Hz, 1H, Ar—H), 7.71 (d, J = 8.6 Hz, 1H, Ar—H), 7.44 (dd, J = 8.6, 1.8 Hz, 1H, Ar—H), 4.46 (t, J = 6.7 Hz, 2H), 3.64 (s, 3H, CH_3), 2.99 (t, J = 6.7 Hz, 2H, CH_2). ^{13}C NMR (100 MHz, DMSO-d_6) δ 171.50, 144.90, 142.76, 135.13, 133.77, 125.85, 125.38, 121.97, 118.50, 116.37, 113.86, 52.08, 48.06, 34.30. ESI-MS: *m/z* 348.7 $[M+H]^+$.

*4.1.11. 2-(4-(6-bromo-1H-benzo[d]imidazol-1-yl)-1H-pyrazol-1-yl)-N,N-dimethylethan-1-amine **(4e)***

67% yield. Oil. ^{1}H NMR (400 MHz, DMSO-d_6) δ 8.52 (s, 1H, Ar—H), 8.45 (s, 1H, Ar—H), 7.96 (s, 1H, Ar—H), 7.75 (d, J = 1.7 Hz, 1H, Ar—H), 7.71 (d, J = 8.6 Hz, 1H, Ar—H), 7.44 (dd, J = 8.6, 1.8 Hz, 1H, Ar—H), 4.29 (t, J = 6.5 Hz, 2H, CH_2), 2.74 (t, J = 6.5 Hz, 2H, CH_2), 2.21 (s, 6H, CH_3). ^{13}C NMR (100 MHz, DMSO-d_6) δ 144.91, 142.79, 135.12, 133.32, 125.82, 125.26, 121.98, 118.42, 116.33, 113.84, 58.79, 50.51, 45.53 (2C). ESI-MS: *m/z* 333.7 $[M+H]^+$.

*4.1.12. 4-(2-(4-(6-Bromo-1H-benzo[d]imidazol-1-yl)-1H-pyrazol-1-yl) ethyl)morpholine **(4f)***

71.4% yield. Oil.^{1}H NMR (400 MHz, DMSO-d_6) δ 8.52 (s, 1H, Ar—H), 8.45 (s, 1H, Ar—H), 7.95 (s, 1H, Ar—H), 7.74 (d, J = 1.7 Hz, 1H, Ar—H), 7.72 (d, J = 8.6 Hz, 1H, Ar—H), 7.44 (dd, J = 8.6, 1.8 Hz, 1H, Ar—H), 4.32 (t, J = 6.4 Hz, 2H, CH_2), 3.59–3.56 (m, 4H, CH_2), 2.77 (t,

Table 3
ADME evaluation of **8i.**

Ligand	Mol.wt. (g/mol)	No. HBA[a]	No. HBD[a]	TPSA(A^2)	cLogp	Lipinski's rule
8i	552.55	9	2	123.95	4.10	Yes; 1 violation: MW > 500

[a] HBA: Hydrogen Bond Acceptor, HBD: Hydrogen Bond Donor.

J = 6.5 Hz, 2H, CH_2), 2.45 (s, 4H, CH_2). ^{13}C NMR (100 MHz, DMSO-d_6) δ 144.92, 142.78, 135.21, 133.49, 125.81, 125.55, 122.00, 118.33, 116.32, 113.79, 66.70 (2C), 58.00, 53.56 (2C), 49.75. ESI-MS: m/z 375.8 $[M+H]^+$.

4.1.13. 2-(4-(6-Bromo-1H-benzo[d]imidazol-1-yl)phenoxy)ethan-1-ol (4g)

69% yield. Oil. ^{1}H NMR (400 MHz, DMSO-d_6) δ 8.52 (s, 1H, Ar—H), 7.73 (d, J = 8.6 Hz, 1H, Ar—H), 7.65 (d, J = 1.4 Hz, 1H, Ar—H), 7.59 (d, J = 8.7 Hz, 2H, Ar—H), 7.44 (dd, J = 8.5, 1.4 Hz, 1H, Ar—H), 7.18 (d, J = 8.8 Hz, 2H, Ar—H), 4.95 (t, J = 4.6 Hz, 1H, OH), 4.09 (t, J = 4.9 Hz, 2H, CH_2), 3.80–3.74 (m, 2H, CH_2). ^{13}C NMR (100 MHz, DMSO-d_6) δ 158.88, 144.99, 143.10, 135.31, 128.58, 126.18, 126.12 (2C), 125.73, 122.07, 116.19 (2C), 113.68, 70.47, 59.98. ESI-MS: m/z 333.0 $[M+H]^+$.

4.1.14. 3-(4-(6-Bromo-1H-benzo[d]imidazol-1-yl)phenoxy)propan-1-ol (4h)

85.7% yield. Oil. ^{1}H NMR (400 MHz, DMSO-d_6) δ 8.51 (s, 1H, Ar—H), 7.73 (d, J = 8.6 Hz, 1H, Ar—H), 7.65 (d, J = 1.7 Hz, 1H, Ar—H), 7.58 (d, J = 8.9 Hz, 2H, Ar—H), 7.44 (dd, J = 8.6, 1.8 Hz, 1H, Ar—H), 7.17 (d, J = 8.9 Hz, 2H, Ar—H), 4.61 (t, J = 5.1 Hz, 1H, OH), 4.14 (t, J = 6.3 Hz, 2H, CH_2), 3.60 (q, J = 6.0 Hz, 2H, CH_2), 1.91 (t, J = 6.3 Hz, 2H, CH_2). ^{13}C NMR (100 MHz, DMSO-d_6) δ 158.86, 144.97, 143.10, 135.31, 128.52, 126.12 (2C), 125.72, 122.06, 116.16, 116.12 (2C), 113.68, 65.52, 57.70, 32.50. ESI-MS: m/z 347.0 $[M+H]^+$.

4.1.15. 4-(4-(6-Bromo-1H-benzo[d]imidazol-1-yl)phenoxy)butan-1-ol (4i)

52.2% yield. Oil. ^{1}H NMR (400 MHz, DMSO-d_6) δ 8.51 (s, 1H, Ar—H), 7.73 (d, J = 8.6 Hz, 1H, Ar—H), 7.65 (d, J = 1.7 Hz, 1H, Ar—H), 7.58 (d, J = 8.9 Hz, 2H, Ar—H), 7.44 (dd, J = 8.6, 1.8 Hz, 1H, Ar—H), 7.17 (d, J = 8.9 Hz, 2H, Ar—H), 4.61 (t, J = 5.1 Hz, 1H, OH), 4.14 (t, J = 6.3 Hz, 2H, CH_2), 3.60 (q, J = 6.0 Hz, 2H, CH_2), 1.91 (t, J = 6.3 Hz, 2H, CH_2). ^{13}C NMR (100 MHz, DMSO-d_6) δ 158.86, 144.97, 143.10, 135.31, 128.52, 126.12 (2C), 125.72, 122.06, 116.16, 116.12 (2C), 113.68, 65.52, 57.70, 32.50. ESI-MS: m/z 347.0 $[M+H]^+$.

4.1.16. Methyl 2-(4-(6-bromo-1H-benzo[d]imidazol-1-yl)phenoxy)acetate (4j)

91.2% yield. mp 167–168 °C. ^{1}H NMR (400 MHz, DMSO-d_6) δ 8.53 (s, 1H, Ar—H), 7.74 (d, J = 8.6 Hz, 1H, Ar—H), 7.66 (d, J = 1.6 Hz, 1H, Ar—H), 7.61 (d, J = 8.9 Hz, 2H, Ar—H), 7.44 (dd, J = 8.6, 1.8 Hz, 1H, Ar—H), 7.18 (d, J = 8.9 Hz, 2H, Ar—H), 4.93 (s, 2H, CH_2), 3.74 (s, 3H, CH_3). ^{13}C NMR (100 MHz, DMSO-d_6) δ 169.54, 157.70, 144.98, 143.12, 135.21, 129.31, 126.08 (2C), 125.77, 122.08, 116.32 (2C), 116.20, 113.69, 65.30, 52.37. ESI-MS: m/z 361.0 $[M+H]^+$.

4.1.17. 4-(2-(4-(6-Bromo-1H-benzo[d]imidazol-1-yl)phenoxy)ethyl) morpholine (4k)

88.7% yield. mp 115–118 °C. ^{1}H NMR (400 MHz, DMSO-d_6) δ 8.52 (s, 1H, Ar—H), 7.73 (d, J = 8.6 Hz, 1H, Ar—H), 7.66–7.63 (m, 1H, Ar—H), 7.58 (d, J = 8.8 Hz, 2H, Ar—H), 7.44 (dd, J = 8.5, 1.7 Hz, 1H, Ar—H), 7.18 (d, J = 8.8 Hz, 2H, Ar—H), 4.19 (t, J = 5.1 Hz, 2H, CH_2), 3.60 (s, 4H, CH_2), 2.81–2.71 (m, 2H, CH_2), 2.56–2.50 (m, 4H, CH_2). ^{13}C NMR (100 MHz, DMSO-d_6) δ 158.58, 144.98, 143.11, 135.31, 128.70, 126.21, 126.12 (2C), 125.73, 122.07, 116.23 (2C), 116.17, 113.68, 66.58 (2C), 66.16, 57.34, 54.02 (2C). ESI-MS: m/z 402.0 $[M+H]^+$.

4.1.18. 4-(3-(4-(6-Bromo-1H-benzo[d]imidazol-1-yl)phenoxy)propyl) morpholine (4l)

92.1% yield. mp 132–133 °C. ^{1}H NMR (400 MHz, DMSO-d_6) δ 8.51 (s, 1H, Ar—H), 7.73 (d, J = 8.6 Hz, 1H, Ar—H), 7.64 (d, J = 1.6 Hz, 1H, Ar—H), 7.58 (d, J = 8.9 Hz, 2H, Ar—H), 7.44 (dd, J = 8.6, 1.8 Hz, 1H, Ar—H), 7.16 (d, J = 8.9 Hz, 2H, Ar—H), 4.10 (t, J = 6.3 Hz, 2H, CH_2), 3.60–3.57 (m, 4H, CH_2), 2.45 (t, J = 7.0 Hz, 2H, CH_2), 2.39 (s, 4H, CH_2), 1.92 (p, J = 6.7 Hz, 2H, CH_2). ^{13}C NMR (100 MHz, DMSO-d_6) δ 158.78, 144.97, 143.11, 135.30, 128.57, 126.12 (2C), 125.73, 122.07, 116.15 (2C), 113.68, 113.63, 66.70 (2C), 66.67, 55.25, 53.84 (2C), 26.27. ESI-MS: m/z 416.0 $[M+H]^+$.

4.1.19. 2-(4-(6-Bromo-1H-benzo[d]imidazol-1-yl)-2-methoxyphenoxy) ethan-1-ol (4m)

55.4% yield. Oil. ^{1}H NMR (400 MHz, DMSO-d_6) δ 7.84 (s, 1H, Ar—H), 7.44 (s, 1H, Ar—H), 7.26 (s, 1H, Ar—H), 7.18 (d, J = 8.6 Hz, 1H, Ar—H), 7.14 (s, 1H, Ar—H), 4.93 (t, J = 5.4 Hz, 1H, OH), 4.07 (t, J = 5.0 Hz, 2H, CH_2), 3.85 (s, 3H, CH_3), 3.77 (q, J = 5.2 Hz, 2H, CH_2). ^{13}C NMR (100 MHz, DMSO-d_6) δ 150.26, 150.07, 148.47, 136.26, 133.96, 129.14, 125.61, 122.41, 116.68, 116.25, 114.23, 114.05, 109.34, 70.97, 60.00, 56.33. ESI-MS: m/z 363.0 $[M+H]^+$.

4.1.20. 3-(4-(6-Bromo-1H-benzo[d]imidazol-1-yl)-2-methoxyphenoxy) propan-1-ol (4n)

73% yield. Oil. ^{1}H NMR (400 MHz, DMSO-d_6) δ 8.53 (s, 1H, Ar—H), 7.73 (d, J = 8.6 Hz, 1H, Ar—H), 7.71–7.70 (m, 1H, Ar—H), 7.44 (dd, J = 8.6, 1.8 Hz, 1H, Ar—H), 7.28–7.25 (m, 1H, Ar—H), 7.17 (s, 1H, Ar—H), 7.16 (s, 1H, Ar—H), 4.59 (t, J = 4.9 Hz, 1H, CH_2), 4.18–4.13 (m, 2H, CH_2), 4.11 (d, J = 6.3 Hz, 2H, CH_2), 3.85 (s, 3H, OCH_3), 1.93 (dp, J = 12.6, 6.3 Hz, 2H). ^{13}C NMR (100 MHz, DMSO-d_6) δ 150.24, 148.46, 145.06, 143.09, 135.35, 128.69, 125.73, 122.02, 116.71, 113.87, 113.80, 109.34, 66.11, 57.81, 56.40, 32.58. ESI-MS: m/z 376.9 $[M+H]^+$.

4.1.21. Methyl 4-((6-bromoquinazolin-4-yl)amino)-2-methoxybenzoate (4o)

68.5% yield. Oil. ^{1}H NMR (400 MHz, DMSO-d_6) δ 8.53 (s, 1H, Ar—H), 7.73 (d, J = 8.6 Hz, 1H, Ar—H), 7.70 (d, J = 1.4 Hz, 1H, Ar—H), 7.44 (dd, J = 8.6, 1.5 Hz, 1H, Ar—H), 7.26 (d, J = 2.0 Hz, 1H, Ar—H), 7.20 (d, J = 8.5 Hz, 1H, Ar—H), 7.16 (dd, J = 8.5, 2.1 Hz, 1H, Ar—H), 4.17 (t, J = 5.8 Hz, 2H, CH_2), 3.85 (s, 3H, OCH_3), 3.62–3.57 (m, 4H, CH_2), 2.74 (t, J = 5.4 Hz, 2H, CH_2), 2.51 (s, 4H, CH_2). ^{13}C NMR (100 MHz, DMSO-d_6) δ 150.31, 148.26, 145.06, 143.09, 135.33, 128.95, 125.75, 122.03, 116.70, 116.18, 114.27, 113.86, 109.44, 67.03, 66.66, 57.44, 56.46, 54.13. ESI-MS: m/z 431.9 $[M+H]^+$.

4.1.22. N-(5-bromo-2-methoxypyridin-3-yl)methanesulfonamide (6a)

Compound **6a** was synthesized according to the procedure described in our previous article [15].

4.1.23. N-(5-bromo-2-methoxypyridin-3-yl)-2,4-difluorobenzenesulfonamide (6b)

Compound **6b** was synthesized according to the procedure described in our previous article [15].

4.1.24. N-(2-methoxy-5-(4,4,5,5-tetramethyl-1,3,2-dioxaborolan-2-yl) pyridin-3-yl)methanesulfonamide (7a)

Compound **7a** was synthesized according to the procedure described in our previous article [15].

4.1.25. 2,4-difluoro-N-(2-methoxy-5-(4,4,5,5-tetramethyl-1,3,2-dioxaborolan-2-yl)pyridin-3-yl)benzenesulfonamide (7b)

Compound **7b** was synthesized according to the procedure described in our previous article [15].

4.1.26. N-(5-(4-((2,4-difluorophenyl)amino)quinazolin-6-yl)-2-methoxypyridin-3-yl)methanesulfonamide (8a)

A solution of the **4a** (0.153 g, 0.5 mmol), **7a** (0.164 g, 0.5 mmol), Cs_2CO_3 (0.33 g, 0.56 mmol) and Bis(triphenylphosphine)palladium(II) Dichloride (0.018 g, 0.025 mmol) in DMF (10 ml) under an atmosphere of N_2 was stirred at 95 °C for 4 h. DMF was removed under reduced pressure and the residue was purified through a column chromatography on silica with chloroform/methanol (V:V 20:1) as a white solid

(0.13 g, 57.0% yield). mp 109–111 °C. ^{1}H NMR (600 MHz, DMSO-d_6) δ 10.16 (s, 1H, NH), 8.50 (s, 1H, Ar−H), 8.45 (s, 1H, Ar−H), 8.33 (d, J = 2.0 Hz, 1H, Ar−H), 8.03 (s, 1H, Ar−H), 7.89 (d, J = 2.1 Hz, 1H, Ar−H), 7.83 (d, J = 8.4 Hz, 1H, Ar−H), 7.75 (s, 1H, Ar−H), 7.53 (d, J = 8.4 Hz, 1H, Ar−H), 5.03 (s, 1H, OH), 4.25 (t, J = 5.5 Hz, 2H, CH_2), 3.96 (s, 3H, OCH_3), 3.82 (t, J = 5.5 Hz, 2H, CH_2), 3.05 (s, 3H, CH_3). ^{13}C NMR (150 MHz, DMSO-d_6) δ 156.59, 144.65, 143.28, 140.59, 134.54, 133.39, 133.01, 131.27, 130.88, 125.41, 122.74, 122.01, 120.70, 118.88, 108.99, 60.37, 55.25, 54.09, 41.06. HRMS (ESI$_+$) m/z calcd for $C_{19}H_{21}N_6O_4S$ $[M+H]^+$, 429.1356; found, 429.1340.

Compounds **8b-8i** were synthesized according to the procedure described in **8a**.

*4.1.27. 2,4-difluoro-N-(5-(1-(1-(2-hydroxyethyl)-1H-pyrazol-4-yl)-1H-benzo[d]imidazol-6-yl)-2-methoxypyridin-3-yl)benzenesulfonamide (**8b**)*

58.6% yield, mp 85–88 °C. ^{1}H NMR (600 MHz, DMSO-d_6) δ 10.28 (s, 1H, NH), 8.49 (s, 1H, Ar−H), 8.44 (s, 1H, Ar−H), 8.31 (s, 1H, Ar−H), 8.03 (s, 1H, Ar−H), 7.87 (s, 1H, Ar−H), 7.82 (d, J = 8.3 Hz, 1H, Ar−H), 7.74 (d, J = 8.2 Hz, 1H, Ar−H), 7.70 (s, 1H, Ar−H), 7.56–7.51 (m, 1H, Ar−H), 7.50–7.48 (m, 1H, Ar−H), 7.17 (t, J = 9.4 Hz, 1H, Ar−H), 5.01 (s, 1H, OH), 4.26 (t, J = 5.6 Hz, 2H, CH_2), 3.85–3.82 (m, 2H, CH_2), 3.66 (s, 3H, OCH_3). ^{13}C NMR (150 MHz, DMSO-d_6) δ 167.41, 166.95, 160.80–158.77 (m), 157.64, 143.09, 135.01, 133.46, 133.31, 132.41, 132.29 (d, J = 10.0 Hz), 132.25, 132.15, 130.80, 129.11, 125.38 (d, J = 28.0 Hz), 123.77, 122.70, 121.87, 120.80, 119.87, 118.85, 112.25 (d, J = 23.3 Hz), 111.11, 109.00, 106.24 (t, J = 22.2 Hz), 60.39, 55.26, 53.76. HRMS (ESI$_+$) m/z calcd for $C_{24}H_{21}F_2N_6O_4S$ $[M+H]^+$, 527.1308; found, 527.1307.

*4.1.28. N-(5-(1-(1-(3-hydroxypropyl)-1H-pyrazol-4-yl)-1H-benzo[d]imidazol-6-yl)-2-methoxypyridin-3-yl)methanesulfonamide (**8c**)*

42.8% yield, mp 170–172 °C. ^{1}H NMR (600 MHz, DMSO-d_6) δ 9.80 (s, 1H, NH), 8.51 (s, 1H, Ar−H), 8.49 (s, 1H, Ar−H), 8.36–8.32 (m, 1H, Ar−H), 8.03 (s, 1H, Ar−H), 7.90 (d, J = 2.0 Hz, 1H, Ar−H), 7.84 (d, J = 8.3 Hz, 1H, Ar−H), 7.75 (s, 1H, Ar−H), 7.54 (d, J = 8.2 Hz, 1H, Ar−H), 4.68 (s, 1H, OH), 4.28 (t, J = 7.0 Hz, 2H, CH_2), 3.96 (s, 3H, OCH_3), 3.47 (t, J = 6.0 Hz, 2H, CH_2), 3.05 (s, 3H, CH_3), 2.01 (p, J = 6.4 Hz, 2H, CH_2). ^{13}C NMR (150 MHz, DMSO-d_6) δ 156.59, 144.67, 143.30, 140.78, 134.51, 133.27, 132.99, 131.41, 130.88, 124.89, 122.55, 122.01, 120.71, 118.92, 108.99, 58.15, 54.11, 49.72, 41.10, 33.45. HRMS (ESI$_+$) m/z calcd for $C_{20}H_{23}N_6O_4S$ $[M+H]^+$, 541.1464; found, 541.1469.

*4.1.29. 2,4-Difluoro-N-(5-(1-(1-(3-hydroxypropyl)-1H-pyrazol-4-yl)-1H-benzo[d]imidazol-6-yl)-2-methoxypyridin-3-yl)benzenesulfonamide (**8d**)*

52.7% yield, mp 98–101 °C. ^{1}H NMR (600 MHz, DMSO-d_6) δ 10.32 (s, 1H, NH), 8.53 (s, 1H, Ar−H), 8.50 (s, 1H, Ar−H), 8.41 (d, J = 2.3 Hz, 1H, Ar−H), 8.05 (s, 1H, Ar−H), 7.94 (d, J = 2.3 Hz, 1H, Ar−H), 7.84 (d, J = 8.4 Hz, 1H, Ar−H), 7.77 (d, J = 2.7 Hz, 1H, Ar−H), 7.74 (d, J = 9.8 Hz, 1H, Ar−H), 7.61–7.56 (m, 1H, Ar−H), 7.52 (dd, J = 8.4, 1.4 Hz, 1H, Ar−H), 7.20 (td, J = 8.5, 2.1 Hz, 1H, Ar−H), 4.68 (s, 1H, OH), 4.28 (t, J = 7.1 Hz, 2H, CH_2), 3.64 (s, 3H, CH_3), 3.47 (t, J = 5.9 Hz, 2H, CH_2), 2.03 (q, J = 6.6 Hz, 2H, CH_2). ^{13}C NMR (150 MHz, DMSO-d_6) δ 165.50 (dd, J = 254.2, 11.7 Hz), 162.75, 159.83 (dd, J = 257.7, 13.1 Hz), 157.65, 144.77, 143.37, 143.14, 135.08, 133.31, 132.42, 132.27 (d, J = 10.4 Hz), 130.80, 125.57 (dd, J = 14.1, 3.2 Hz), 124.91, 121.88, 120.78, 119.85, 118.88, 112.24 (d, J = 23.0 Hz), 109.00, 106.24 (t, J = 25.9 Hz), 58.16, 53.76, 49.73, 33.46. HRMS (ESI$_+$) m/z calcd for $C_{25}H_{23}F_2N_6O_4S$ $[M+H]^+$, 541.1464; found, 541.1469.

*4.1.30. Methyl 2-(4-(6-(5-((2,4-difluorophenyl)sulfonamido)-6-methoxypyridin-3-yl)-1H-benzo[d]imidazol-1-yl)-1H-pyrazol-1-yl) acetate (**8e**)*

53.4% yield, mp 103–105 °C. ^{1}H NMR (600 MHz, DMSO-d_6) δ 10.34 (s, 1H, NH), 8.55 (s, 1H, Ar−H), 8.52 (s, 1H, Ar−H), 8.28 (s, 1H, Ar−H), 8.11 (s, 1H, Ar−H), 7.85 (s, 1H, Ar−H), 7.83 (d, J = 8.4 Hz, 1H, Ar−H), 7.75 (q, J = 8.5 Hz, 1H, Ar−H), 7.67 (s, 1H, Ar−H), 7.51 (d, J = 9.1 Hz, 1H, Ar−H), 7.49 (d, J = 9.5 Hz, 1H, Ar−H), 7.19–7.13 (m, 2H, Ar−H), 5.22 (s, 2H, CH_2), 3.73 (s, 3H, OCH_3), 3.66 (s, 3H, OCH_3). ^{13}C NMR (150 MHz, DMSO-d_6) δ 168.90, 166.15–164.09 (m), 162.56, 159.77 (dd, J = 257.1, 13.4 Hz), 157.56, 144.60, 143.30, 141.26 (d, J = 5.7 Hz), 134.44, 134.22 (2C), 132.93, 132.20 (d, J = 10.7 Hz), 130.66, 126.53, 126.18, 121.94, 120.82, 119.58, 112.02 (d, J = 21.1 Hz), 108.73, 106.08 (t, J = 25.9 Hz), 53.65, 53.53, 52.83. HRMS (ESI$_+$) m/z calcd for $C_{25}H_{21}F_2N_6O_5S$ $[M+H]^+$, 555.1257; found, 555.1255.

*4.1.31. Methyl 3-(4-(6-(5-((2,4-difluorophenyl)sulfonamido)-6-methoxypyridin-3-yl)-1H-benzo[d]imidazol-1-yl)-1H-pyrazol-1-yl) propanoate (**8f**)*

61.9% yield, mp 110–112 °C. ^{1}H NMR (600 MHz, DMSO-d_6) δ 10.32 (s, 1H, NH), 8.52 (s, 1H, Ar−H), 8.51 (s, 1H, Ar−H), 8.41 (d, J = 2.2 Hz, 1H, Ar−H), 8.05 (s, 1H, Ar−H), 7.93 (d, J = 2.2 Hz, 1H, Ar−H), 7.84 (d, J = 8.4 Hz, 1H, Ar−H), 7.76 (d, J = 8.5 Hz, 1H, Ar−H), 7.74 (d, J = 5.2 Hz, 1H, Ar−H), 7.61–7.56 (m, 1H, Ar−H), 7.52 (dd, J = 8.4, 1.4 Hz, 1H, Ar−H), 7.20 (td, J = 8.5, 2.2 Hz, 1H, Ar−H), 4.48 (t, J = 6.7 Hz, 2H, CH_2), 3.64 (s, 3H, OCH_3), 3.63 (s, 3H, OCH_3), 3.01 (t, J = 6.7 Hz, 2H, CH_2). ^{13}C NMR (150 MHz, DMSO-d_6) δ 171.52, 166.44–164.50 (m), 162.75, 159.83 (dd, J = 257.8, 13.3 Hz), 157.68, 144.69, 143.37, 143.07, 135.07, 134.49, 133.66, 132.45, 132.31, 132.24, 130.77, 125.18, 121.89, 120.81, 118.96, 112.23 (d, J = 22.0 Hz), 108.95, 106.23 (t, J = 26.1 Hz), 53.75, 52.09, 48.04, 34.32. HRMS (ESI$_+$) m/z calcd for $C_{26}H_{23}F_2N_6O_5S$ $[M+H]^+$, 569.1413; found, 569.1392.

*4.1.32. N-(5-(1-(1-(2-(dimethylamino)ethyl)-1H-pyrazol-4-yl)-1H-benzo[d]imidazol-6-yl)-2-methoxypyridin-3-yl)-2,4-difluorobenzenesulfonamide (**8g**)*

42.6% yield, mp 80–82 °C. ^{1}H NMR (600 MHz, DMSO-d_6) δ 11.49 (s, 1H, NH), 8.53 (s, 2H, Ar−H), 8.37 (d, J = 2.1 Hz, 1H, Ar−H), 8.06 (s, 1H, Ar−H), 7.91 (d, J = 2.3 Hz, 1H, Ar−H), 7.84 (d, J = 8.4 Hz, 1H, Ar−H), 7.75–7.73 (m, 1H, Ar−H), 7.72 (d, J = 7.4 Hz, 1H, Ar−H), 7.57–7.54 (m, 1H, Ar−H), 7.52 (dd, J = 8.4, 1.4 Hz, 1H, Ar−H), 7.20 (dt, J = 8.4, 4.3 Hz, 1H, Ar−H), 4.38 (d, J = 6.2 Hz, 2H, CH_2), 3.65 (s, 3H, OCH_3), 2.93 (d, J = 7.1 Hz, 2H, CH_2), 1.91 (s, 6H, NCH_3). ^{13}C NMR (100 MHz, DMSO-d_6) δ 165.33 (dd, J = 253.9, 11.7 Hz), 159.81 (dd, J = 257.3, 13.4 Hz), 157.55, 142.05, 133.89, 133.47, 132.67, 132.25 (d, J = 10.7 Hz), 130.73, 125.83, 125.37, 125.25, 121.93, 121.85, 121.16, 120.77, 118.98, 118.52, 116.35, 113.84, 112.22, 111.98, 108.85, 106.11 (t, J = 26.1 Hz), 58.35, 53.69, 50.03, 45.08 (2C). HRMS (ESI$_+$) m/z calcd for $C_{25}H_{23}F_2N_6O_4S$ $[M+H]^+$, 554.1780; found, 554.1780.

*4.1.33. 2,4-Difluoro-N-(2-methoxy-5-(1-(1-(2-morpholinoethyl)-1H-pyrazol-4-yl)-1H-benzo[d]imidazol-6-yl)pyridin-3-yl)benzenesulfonamide (**8h**)*

53.2% yield, mp 66–68 °C. ^{1}H NMR (600 MHz, DMSO-d_6) δ 10.32 (s, 1H, NH), 8.53 (s, 1H, Ar−H), 8.51 (s, 1H, Ar−H), 8.39 (d, J = 2.1 Hz, 1H, Ar−H), 8.04 (s, 1H, Ar−H), 7.93 (d, J = 2.1 Hz, 1H, Ar−H), 7.84 (d, J = 8.4 Hz, 1H, Ar−H), 7.77–7.73 (m, 1H, Ar−H), 7.72 (s, 1H, Ar−H), 7.60–7.56 (m, 1H, Ar−H), 7.54–7.50 (m, 1H, Ar−H), 7.22–7.18 (m, 1H, Ar−H), 4.35 (t, J = 6.3 Hz, 2H), 3.64 (s, 3H, OCH_3), 3.56 (s, 4H, CH_2), 2.88–2.78 (m, 2H, CH_2), 2.51 (s, 4H, CH_2). ^{13}C NMR (150 MHz, DMSO-d_6) δ 165.49 (dd, J = 253.8, 11.7 Hz), 159.83 (dd, J = 257.4, 13.3 Hz), 157.65, 144.74, 143.39, 143.07, 135.03, 134.56, 133.41, 132.45, 132.27 (d, J = 11.1 Hz), 130.81, 125.57 (d, J = 13.2 Hz), 125.24, 121.90, 120.82, 119.90, 118.90, 112.25 (d, J = 21.7 Hz), 108.95, 106.23 (t, J = 25.8 Hz), 66.52 (2C), 57.93, 53.76, 53.50 (2C), 40.89. HRMS (ESI$_+$) m/z calcd for $C_{28}H_{28}F_2N_7O_4S$ $[M+H]^+$, 596.1886; found, 596.1880.

*4.1.34. 2,4-Difluoro-N-(5-(1-(4-(2-hydroxyethoxy)phenyl)-1H-benzo[d]imidazol-6-yl)-2-methoxypyridin-3-yl)benzenesulfonamide **(8i)***

53.9% yield, mp 104–106 °C. ^{1}H NMR (600 MHz, DMSO-d_6) δ 10.30 (s, 1H, NH), 8.53 (s, 1H, Ar−H), 8.35 (d, J = 2.4 Hz, 1H, Ar−H), 7.88 (d, J = 2.3 Hz, 1H, Ar−H), 7.85 (d, J = 8.4 Hz, 1H, Ar−H), 7.74 (q, J = 8.2, 7.8 Hz, 1H, Ar−H), 7.66 (d, J = 2.4 Hz, 1H, Ar−H), 7.66–7.64 (m, 2H, Ar−H), 7.60–7.55 (m, 1H, Ar−H), 7.52 (dd, J = 8.4, 1.7 Hz, 1H, Ar−H), 7.20 (d, J = 8.8 Hz, 2H, Ar−H), 7.17 (d, J = 10.1 Hz, 1H, Ar−H), 4.95 (t, J = 5.5 Hz, 1H, OH), 4.10 (t, J = 4.9 Hz, 2H, CH_2), 3.77 (q, J = 4.9 Hz, 2H, CH_2), 3.63 (s, 3H, OCH_3). ^{13}C NMR (100 MHz, DMSO-d_6) δ 165.50 (dd, J = 253.9, 11.9 Hz), 159.81 (dd, J = 257.0, 13.4 Hz), 158.75, 157.58, 144.83, 143.74, 142.92, 134.76, 132.33, 132.20, 130.88, 129.03, 126.05 (2C), 125.89, 125.60 (d, J = 13.8 Hz), 121.84, 120.87, 119.95, 116.20 (2C), 112.25 (dd, J = 22.0, 3.0 Hz), 108.89, 106.23 (t, J = 26.3 Hz), 70.47, 60.02, 53.77. HRMS (ESI$_+$) m/z calcd for $C_{27}H_{23}F_2N_4O_5S$ $[M+H]^+$, 553.1352; found, 553.1349.

*4.1.35. 2,4-Difluoro-N-(5-(1-(4-(2-hydroxyethoxy)-3-methoxyphenyl)-1H-benzo[d]imidazol-6-yl)-2-methoxypyridin-3-yl)benzenesulfonamide **(8j)***

42.7% yield, mp 58–60 °C. ^{1}H NMR (600 MHz, DMSO-d_6) δ 10.30 (s, 1H, NH), 8.53 (d, J = 13.5 Hz, 1H, Ar−H), 8.26 (d, J = 12.2 Hz, 1H, Ar−H), 7.84 (s, 1H, Ar−H), 7.83 (s, 1H, Ar−H), 7.75–7.71 (m, 1H, Ar−H), 7.67 (d, J = 12.3 Hz, 1H, Ar−H), 7.52 (s, 1H, Ar−H), 7.48 (s, 1H, Ar−H), 7.32 (d, J = 11.3 Hz, 1H, Ar−H), 7.23 (d, J = 8.5 Hz, 1H, Ar−H), 7.20 (d, J = 8.2 Hz, 1H, Ar−H), 7.14–7.10 (m, 1H, Ar−H), 4.95–4.91 (m, 1H, OH), 4.09–4.06 (m, 2H, CH_2), 3.87 (s, 3H, OCH_3), 3.78–3.75 (m, 2H, CH_2), 3.66 (s, 3H, OCH_3). ^{13}C NMR (150 MHz, DMSO-d_6) δ 165.21 (dd, J = 252.2, 11.1 Hz), 159.76 (dd, J = 257.2, 13.5 Hz), 157.47, 150.22, 148.25, 144.83, 143.66, 134.69, 132.21, 132.14, 130.75, 129.25, 126.17 (dd, J = 23.6, 7.1 Hz), 121.77, 120.81, 116.50, 114.03, 112.04 (d, J = 22.3 Hz), 109.15, 108.95, 106.12 (t, J = 26.1 Hz), 70.94, 63.24, 56.30, 53.69. HRMS (ESI$_+$) m/z calcd for $C_{28}H_{25}F_2N_4O_6S$ $[M+H]^+$, 583.1457; found, 541.1469.

*4.1.36. N-(5-(1-(4-(3-hydroxypropoxy)phenyl)-1H-benzo[d]imidazol-6-yl)-2-methoxypyridin-3-yl)methanesulfonamide **(8k)***

47.6% yield, mp 77–79 °C. ^{1}H NMR (600 MHz, DMSO-d_6) δ 9.35 (s, 1H, NH), 8.51 (s, 1H, Ar−H), 8.33 (d, J = 2.2 Hz, 1H, Ar−H), 7.88 (d, J = 2.1 Hz, 1H, Ar−H), 7.85 (d, J = 8.4 Hz, 1H, Ar−H), 7.66 (s, 1H, Ar−H), 7.64 (d, J = 8.8 Hz, 2H, Ar−H), 7.56–7.53 (m, 1H, Ar−H), 7.17 (d, J = 8.8 Hz, 2H, Ar−H), 4.62 (t, J = 4.8 Hz, 1H, OH), 4.13 (t, J = 6.3 Hz, 2H, CH_2), 3.96 (s, 3H, OCH_3), 3.59 (q, J = 5.5 Hz, 2H, CH_2), 3.07 (s, 3H, CH_3), 1.91 (p, J = 6.2 Hz, 2H, CH_2). ^{13}C NMR (150 MHz, DMSO-d_6) δ 158.66, 156.56, 144.76, 143.67, 141.41, 134.64, 132.70, 132.02, 130.98, 128.96, 125.99 (2C), 121.98, 121.62, 120.81, 116.08 (2C), 108.94, 65.46, 57.69, 54.19, 41.19, 32.51. HRMS (ESI$_+$) m/z calcd for $C_{23}H_{25}N_4O_5S$ $[M+H]^+$, 469.1540; found, 469.1534.

*4.1.37. 2,4-Difluoro-N-(5-(1-(4-(3-hydroxypropoxy)phenyl)-1H-benzo[d]imidazol-6-yl)-2-methoxypyridin-3-yl)benzenesulfonamide **(8l)***

51.2.0% yield, mp 72–74 °C. ^{1}H NMR (600 MHz, DMSO-d_6) δ 10.30 (s, 1H, NH), 8.53 (s, 1H, Ar−H), 8.35 (d, J = 2.2 Hz, 1H, Ar−H), 7.88 (d, J = 2.1 Hz, 1H, Ar−H), 7.86 (d, J = 8.4 Hz, 1H, Ar−H), 7.77–7.73 (m, 1H, Ar−H), 7.66 (s, 1H, Ar−H), 7.66–7.61 (m, 2H, Ar−H), 7.56 (d, J = 8.8 Hz, 1H, Ar−H), 7.54–7.51 (m, 1H, Ar−H), 7.19 (d, J = 8.8 Hz, 2H, Ar−H), 7.16 (d, J = 2.3 Hz, 1H, Ar−H), 4.62 (t, J = 5.0 Hz, 1H, OH), 4.15 (d, J = 6.3 Hz, 2H, CH_2), 3.64 (s, 3H, OCH_3), 3.60 (q, J = 6.6, 5.7 Hz, 2H, CH_2), 1.92 (p, J = 6.2 Hz, 2H, CH_2). ^{13}C NMR (150 MHz, DMSO-d_6) δ 165.48 (dd, J = 253.9, 11.6 Hz), 160.79–160.54 (m), 158.96 (d, J = 13.7 Hz), 158.70, 157.59, 144.82, 143.73, 142.94, 134.83, 134.71, 132.31, 132.22, 130.87, 128.94, 126.05 (2C), 125.58 (dd, J = 14.3, 2.9 Hz), 121.84, 120.86, 119.92, 116.09 (2C), 112.24 (d, J = 22.2 Hz), 108.89, 106.23 (t, J = 26.2 Hz), 65.49, 57.71, 53.76, 32.53. HRMS (ESI$_+$) m/z calcd for $C_{28}H_{25}F_2N_4O_5S$ $[M+H]^+$, 567.1508; found, 567.1502.

*4.1.38. 2,4-Difluoro-N-(5-(1-(4-(3-hydroxypropoxy)-3-methoxyphenyl)-1H-benzo[d]imidazol-6-yl)-2-methoxypyridin-3-yl)benzenesulfonamide **(8m)***

52.6% yield, mp 69–71 °C. ^{1}H NMR (600 MHz, DMSO-d_6) δ 10.30 (s, 1H, NH), 8.56 (s, 1H, Ar−H), 8.39–8.32 (m, 1H, Ar−H), 7.90 (s, 1H, Ar−H), 7.86 (d, J = 8.3 Hz, 1H, Ar−H), 7.78–7.73 (m, 1H, Ar−H), 7.71 (s, 1H, Ar−H), 7.57 (d, J = 9.4 Hz, 1H, Ar−H), 7.54 (d, J = 8.8 Hz, 1H, Ar−H), 7.36–7.31 (m, 1H, Ar−H), 7.28–7.23 (m, 1H, Ar−H), 7.20 (d, J = 10.8 Hz, 1H, Ar−H), 7.17 (d, J = 9.5 Hz, 1H, Ar−H), 4.59 (s, 1H, OH), 4.15–4.12 (m, 2H, CH_2), 3.87 (s, 3H, OCH_3), 3.65 (s, 3H, OCH_3), 3.60 (t, J = 5.5 Hz, 2H, CH_2), 3.49–3.43 (m, 2H, CH_2). ^{13}C NMR (150 MHz, DMSO-d_6) δ 165.50 (dd, J = 254.1, 11.7 Hz), 160.81–158.67 (m), 157.50, 150.21, 148.28, 144.84, 143.59, 142.81, 134.68, 134.56, 132.29, 132.21, 130.79, 129.06, 125.66–125.15 (m), 121.85, 120.83, 119.95, 116.59, 113.82, 112.24 (d, J = 21.8 Hz), 109.13, 109.01, 106.19 (t, J = 26.3 Hz), 66.09, 57.85, 56.37, 53.80, 32.53. HRMS (ESI$_+$) m/z calcd for $C_{29}H_{27}F_2N_4O_6S$ $[M+H]^+$, 597.1614; found, 597.1610.

*4.1.39. 2,4-Difluoro-N-(5-(1-(4-(4-hydroxybutoxy)phenyl)-1H-benzo[d]imidazol-6-yl)-2-methoxypyridin-3-yl)benzenesulfonamide **(8n)***

47.2% yield, mp 101–103 °C. ^{1}H NMR (600 MHz, DMSO-d_6) δ 10.31 (s, 1H, NH), 8.57 (s, 1H, Ar−H), 8.35 (d, J = 2.3 Hz, 1H, Ar−H), 7.88 (d, J = 2.3 Hz, 1H, Ar−H), 7.86 (d, J = 8.4 Hz, 1H, Ar−H), 7.77–7.72 (m, 1H, Ar−H), 7.67 (s, 1H, Ar−H), 7.65 (s, 2H, Ar−H), 7.59–7.55 (m, 1H, Ar−H), 7.54 (dd, J = 8.4, 1.5 Hz, 1H, Ar−H), 7.19 (d, J = 2.9 Hz, 1H, Ar−H), 7.17 (d, J = 4.3 Hz, 2H, Ar−H), 4.49 (s, 1H, OH), 4.09 (t, J = 6.5 Hz, 2H, CH_2), 3.64 (s, 3H, OCH_3), 3.48 (t, J = 6.4 Hz, 2H, CH_2), 1.80 (p, J = 6.6 Hz, 2H, CH_2), 1.61 (p, J = 6.5 Hz, 2H, CH_2). ^{13}C NMR (150 MHz, DMSO-d_6) δ 165.48 (dd, J = 253.9, 11.5 Hz), 159.81 (dd, J = 257.8, 13.1 Hz), 158.73, 157.61, 144.80, 143.41, 142.97, 134.85, 132.40, 132.29, 132.22, 130.83, 128.86, 126.08, 125.53, 121.95, 120.74, 119.91, 116.10, 112.24 (d, J = 22.3 Hz), 108.97, 106.23 (t, J = 26.0 Hz), 68.34, 60.84, 53.76, 29.43, 25.88. HRMS (ESI$_+$) m/z calcd for $C_{29}H_{27}F_2N_4O_5S$ $[M+H]^+$, 581.1665; found, 581.1679.

*4.1.40. Methyl 2-(4-(6-(5-((2,4-difluorophenyl)sulfonamido)-6-methoxypyridin-3-yl)-1H-benzo[d]imidazol-1-yl)phenoxy)acetate **(8o)***

68.6% yield, mp 78–80 °C. ^{1}H NMR (600 MHz, DMSO-d_6) δ 10.30 (s, 1H, NH), 8.55 (s, 1H, Ar−H), 8.35 (d, J = 2.3 Hz, 1H, Ar−H), 7.88 (d, J = 2.3 Hz, 1H, Ar−H), 7.86 (d, J = 8.4 Hz, 1H, Ar−H), 7.77–7.72 (m, 1H, Ar−H), 7.70–7.67 (m, 2H, Ar−H), 7.66–7.64 (m, 1H, Ar−H), 7.59–7.55 (m, 1H, Ar−H), 7.53 (dd, J = 8.4, 1.6 Hz, 1H, Ar−H), 7.20 (d, J = 8.9 Hz, 2H, Ar−H), 7.17 (dd, J = 8.5, 2.2 Hz, 1H, Ar−H), 4.94 (s, 2H, CH_2), 3.74 (s, 3H, OCH_3), 3.64 (s, 3H, OCH_3). ^{13}C NMR (150 MHz, DMSO-d_6) δ 169.57, 166.44–164.49 (m), 159.81 (dd, J = 257.4, 13.4 Hz), 157.61, 157.53, 144.83, 143.73, 142.99, 134.89, 134.59, 132.36, 132.26 (d, J = 11.0 Hz), 130.86, 129.74, 125.98 (2C), 125.66–125.48 (m), 121.90, 120.88, 119.89, 116.29 (2C), 112.25 (d, J = 23.8 Hz), 108.93, 106.24 (t, J = 26.1 Hz), 65.29, 53.76, 52.35. HRMS (ESI$_+$) m/z calcd for $C_{28}H_{23}F_2N_4O_6S$ $[M+H]^+$, 581.1301; found, 581.1302.

*4.1.41. 2,4-Difluoro-N-(2-methoxy-5-(1-(4-(2-morpholinoethoxy)phenyl)-1H-benzo[d]imidazol-6-yl)pyridin-3-yl)benzenesulfonamide **(8p)***

47.6% yield, mp 68–70 °C.^{1}H NMR (600 MHz, DMSO-d_6) δ 10.32 (s, 1H, NH), 8.52 (d, J = 4.4 Hz, 1H, Ar−H), 8.38–8.30 (m, 1H, Ar−H), 7.89–7.86 (m, 1H, Ar−H), 7.75–7.72 (m, 1H, Ar−H), 7.66 (d, J = 8.8 Hz, 2H, Ar−H), 7.64 (s, 1H, Ar−H), 7.59 (d, J = 8.6 Hz, 1H, Ar−H), 7.56 (d, J = 9.2 Hz, 1H, Ar−H), 7.53 (d, J = 8.3 Hz, 1H, Ar−H), 7.23–7.19 (m, 2H, Ar−H), 7.17 (d, J = 7.1 Hz, 1H, Ar−H), 4.24–4.19 (m, 2H, CH_2), 3.64 (s, 3H, OCH_3), 3.61 (s, 4H, CH_2), 2.79–2.75 (m, 2H, CH_2), 2.53 (s, 4H, CH_2). ^{13}C NMR (150 MHz, DMSO-d_6) δ 165.46 (dd, J = 254.1, 11.1 Hz), 162.74, 161.07–158.74 (m), 158.56, 158.42,

157.56, 144.94, 144.79, 143.72, 142.77, 134.70, 134.62, 132.36, 132.29, 132.22, 130.86, 129.12, 126.09, 126.03 (2C), 116.20 (2C), 112.21 (d, J = 21.0 Hz), 108.87, 106.21 (t, J = 26.3 Hz), 66.54 (2C), 66.11, 57.34, 54.00 (2C), 53.75. HRMS (ESI_+) m/z calcd for $C_{31}H_{29}F_2N_5NaO_5S$ $[M+Na]^+$, 644.1750; found, $[M+H]^+$, 644.1749.

4.1.42. 2,4-Difluoro-N-(2-methoxy-5-(1-(3-methoxy-4-(2-morpholinoethoxy)phenyl)-1H-benzo[d]imidazol-6-yl)pyridin-3-yl) benzenesulfonamide (**8q**)

41.8% yield, mp 92–94 °C. ^1H NMR (600 MHz, DMSO-d_6) δ 10.30 (s, 1H, NH), 8.55 (s, 1H, Ar−H), 8.34 (s, 1H, Ar−H), 7.89 (s, 1H, Ar−H), 7.86 (d, J = 8.3 Hz, 1H, Ar−H), 7.74 (q, J = 8.1 Hz, 1H, Ar−H), 7.70 (s, 1H, Ar−H), 7.57 (d, J = 8.8 Hz, 1H, Ar−H), 7.53 (d, J = 8.7 Hz, 1H, Ar−H), 7.33 (s, 1H, Ar−H), 7.24 (d, J = 8.1 Hz, 1H, Ar−H), 7.22 (d, J = 8.5 Hz, 1H, Ar−H), 7.17 (t, J = 7.6 Hz, 1H, Ar−H), 4.19 (t, J = 5.4 Hz, 2H, CH_2), 3.87 (s, 3H, OCH_3), 3.65 (s, 3H, OCH_3), 3.60 (s, 4H, CH_2), 2.77 (t, J = 4.9 Hz, 2H, CH_2), 2.54 (s, 4H, CH_2). ^{13}C NMR (150 MHz, DMSO-d_6) δ 165.45 (dd, J = 253.8, 11.6 Hz), 159.80 (dd, J = 257.5, 13.3 Hz), 157.52, 150.29, 148.01, 144.88, 143.73, 142.72, 134.68, 134.62, 132.31, 132.20, 130.82, 129.41, 125.61 (d, J = 12.0 Hz), 121.80, 120.85, 120.13, 116.51, 114.29, 112.22 (d, J = 23.8 Hz), 109.23, 109.05, 106.23 (t, J = 25.9 Hz), 66.91, 66.56, 57.40, 56.43, 54.07, 53.77. HRMS (ESI_+) m/z calcd for $C_{32}H_{32}F_2N_5O_6S$ $[M+H]^+$, 652.2036; found, 652.2035.

4.1.43. N-(2-methoxy-5-(1-(4-(3-morpholinopropoxy)phenyl)-1H-benzo[d]imidazol-6-yl)pyridin-3-yl)methanesulfonamide (**8r**)

45.8% yield, mp 94–96 °C. ^1H NMR (600 MHz, DMSO-d_6) δ 9.42 (s, 1H, NH), 8.52 (s, 1H, Ar−H), 8.32 (d, J = 2.0 Hz, 1H, Ar−H), 7.88 (d, J = 2.0 Hz, 1H, Ar−H), 7.86 (d, J = 8.4 Hz, 1H, Ar−H), 7.66 (d, J = 5.6 Hz, 2H, Ar−H), 7.64 (s, 1H, Ar−H), 7.55 (d, J = 8.3 Hz, 1H, Ar−H), 7.17 (d, J = 8.8 Hz, 2H, Ar−H), 4.11 (t, J = 6.2 Hz, 2H, CH_2), 3.96 (s, 3H, OCH_3), 3.58 (s, 4H, CH_2), 3.07 (s, 3H, CH_3), 2.45 (t, J = 7.1 Hz, 2H, CH_2), 2.43–2.33 (m, 4H, CH_2), 1.94–1.90 (m, 2H, CH_2). ^{13}C NMR (150 MHz, DMSO-d_6) δ 158.59, 156.55, 144.75, 143.68, 141.27, 134.64, 132.74, 131.88, 130.97, 129.01, 125.99 (2C), 121.98, 121.79, 120.82, 116.11 (2C), 108.93, 66.67 (2C), 55.26, 54.17, 53.85 (2C), 41.17, 26.30. HRMS (ESI_+) m/z calcd for $C_{27}H_{32}N_5O_5S$ $[M+H]^+$, 538.2199; found, 538.2099.

4.1.44. 2,4-Difluoro-N-(2-methoxy-5-(1-(4-(3-morpholinopropoxy) phenyl)-1H-benzo[d]imidazol-6-yl)pyridin-3-yl)benzenesulfonamide (**8s**)

42.5% yield, mp 79–81 °C. ^1H NMR (600 MHz, DMSO-d_6) δ 10.30 (s, 1H, NH), 8.52 (s, 1H, Ar−H), 8.33 (d, J = 2.3 Hz, 1H, Ar−H), 7.87–7.84 (m, 2H, Ar−H), 7.76–7.72 (m, 1H, Ar−H), 7.66 (s, 1H, Ar−H), 7.65 (s, 1H, Ar−H), 7.63 (s, 1H, Ar−H), 7.58–7.54 (m, 1H, Ar−H), 7.52 (dd, J = 8.4, 1.4 Hz, 1H, Ar−H), 7.18 (d, J = 8.9 Hz, 2H, Ar−H), 7.16 (dd, J = 8.5, 2.2 Hz, 1H, Ar−H), 4.12 (t, J = 6.3 Hz, 2H, CH_2), 3.64 (s, 3H, OCH_3), 3.61–3.59 (m, 4H, CH_2), 2.51–2.50 (m, 4H, CH_2), 2.45 (s, 2H, CH_2), 1.95 (q, J = 6.7 Hz, 2H, CH_2). ^{13}C NMR (150 MHz, DMSO-d_6) δ 172.47, 165.43 (dd, J = 254.0, 11.6 Hz), 162.75, 159.80 (dd, J = 257.6, 13.3 Hz), 158.58, 157.57, 144.84, 143.72, 142.67, 134.58, 132.36, 130.84, 129.02, 126.11, 126.06 (2C), 125.87–125.51 (m), 121.83, 120.87, 120.24, 116.11 (2C), 112.20 (d, J = 22.1 Hz), 108.87, 106.22 (t, J = 26.2 Hz), 66.59, 66.43 (2C), 55.15, 53.66 (2C), 26.07. HRMS (ESI_+) m/z calcd for $C_{32}H_{32}F_2N_5O_5S$ $[M+H]^+$, 636.2087; found, 636.2114.

4.2. Biological assay methods

4.2.1. Cell culture

T47D, HCT116 and MCF-7 cells were purchased from the American Type Culture Collection (Manassas, VA, USA). Cells were grown in DMEM (T47D, MCF-7) or RPMI1640 (HCT116) supplemented with 10% FBS and antibiotics-antimycotics (PSF; 100 units/mL penicillin G sodium, 100 μg/ml streptomycin and 250 ng/ml amphotericin B) in a humidified incubator containing 5% CO_2 at 37 °C.

4.2.2. Antiproliferative activity

The activity was evaluated using the sulforhodamine B (SRB) cellular protein-staining method with minor modifications. Briefly, cells were treated with various concentrations of compounds in 96-well plates and incubated at 37 °C in a humidified atmosphere with 5% CO_2 for 72 h. After treatment, the cells were fixed with 10% TCA solution, and cell viability was determined with SRB assay. The percentage of cell-growth inhibition was calculated using the formulae below. The IC_{50} values were calculated using a non-linear regression analysis (percent growth versus concentration). Percent growth inhibition = 100–100 × $(OD_{sample} - OD_{Day0})/(OD_{neg\ control} - OD_{Day0})$.

4.2.3. PI3K enzymatic activity assay

The PI3K enzymatic activity were tested at Shanghai ChemPartner Co., Ltd.

4.2.4. Colony formation assay

HCT116 cells were seeded in a 6-well plates with a density of 3×10^3 cells/well and then were cultured with different concentrations (0, 1.0, 2.5, 5.0 μM) of **8i** about 2 weeks. Cells were fixed by ethanol and stained with crystal violet.

4.2.5. Transwell and wound healing assays

For the invasion assay, dilute matrigel with DMEM (1:6) and then placed 60 μl in the upper chamber of the 24-well plate, which was incubated at 37 °C in a humidified atmosphere with 5% CO_2 for 12–24 h. HCT116 cells were resuspended in DMEM without serum (2×10^4/200 μl), added 100 μl cells and 100 μl **8i** to each upper chamber, added 700 μl DMEM with 10% FBS to each lower chamber, and incubated at 37 °C in a humidified atmosphere with 5% CO_2 for 48 h. Cells that crossed to the underside of the membrane were fixed in 70% ethanol, infiltrated with 100% methanol, then stained with 0.1% crystal violet, and observed and taked pictures under microscope. For wound healing assay, 2 ml HCT116 cells with a density of 5×10^5/well were placed in 6-well plate and incubated at 37 °C in a humidified atmosphere with 5% CO_2 for 12–24 h and grown to confluency. Then we used 200 μl tip to scratch cell monolayers to create a cell-free zone. Washed each well 3 times with PBS buffer and added 2 ml **8i** to each well, and then incubated at 37 °C in a humidified atmosphere with 5% CO_2 for 48 h. Photographed at 0 h, 24 h, 48 h under the microscope to observe cell migration.

4.2.6. Annexin V-FITC and propidium iodide (PI) double staining assay

Apoptotic cells were quantified with an annexin-V-fluorescein isothiocyanate (FITC)/propidium iodide (PI) apoptosis detection kit. HCT116 cells were seeded in a 6-well plate (3×10^5 cells/well) and treated with **8i** mentioned above. At the end of treatments, the cells were washed by PBS and harvested by trypsin without EDTA. Annexin-V/PI double staining was performed according to the manufacturers' instructions. Stained cells were analyzed with a flow cytometer. Annexin-V-/PI- was used to represent viable cells, Annexin-V+/PI- was used to represent early apoptotic cells, Annexin-V+/PI+ was used to represent late apoptotic cells.

4.2.7. Hoechst33342 staining assay

Hoechst33342 staining assay was performed according to manufacturers' instructions. HCT116 cells were seeded in a 6-well plate (3×10^5 cells/well) and treated with **8i** mentioned above. At the end of treatments, the cells were washed by PBS 2 times, and then we added 1 ml Hoechst 33,342 (c = 10 μg/ml) to each well, which was incubated at 37 °C in a humidified atmosphere with 5% CO_2 for 15 min. The cells were washed by PBS 2 times and we added 1 ml PBS to each well. Photographed under the microscope to observe cell morphology and apoptosis.

4.2.8. Western blot analysis

Cells were seeded into 100 mm dishes and allowed to adhere overnight prior to treatment. After treatment, cells were collected and lysed in RIPA buffer (50 mM Tris-HCl, pH 8.0, 150 mM NaCl, 1% NP-40, 0.5% sodium deoxycholate, 0.1% SDS), and centrifuged at 13,000 r for 15 min in the 4 ˚C centrifuge. Supernatants were collected, and the total protein concentration was quantified with a bicinchoninic acid (BCA) assay kit. The protein concentration was determined, equal amounts of proteins (30 μg) were loaded onto SDS-PAGE gels, and separated proteins were transferred to PVDF membranes. After blocking with 5% BSA at room temperature for 2 h, the membranes were incubated with primary antibodies against AKT and p-AKT, a monoclonal antibody against β-actin was used as a protein loading control. The membranes were washed three times with TBST buffer for 30 min, 10 min at a time, then incubated with HRP-conjugated secondary antibody for 2 h. After washing with the TBST buffer again, membranes were scanned with the Odyssey Infrared Imaging System.

4.2.9. Molecular docking studies

The specific operation steps are shown in our previous work [15].

Acknowledgments

Financial supported by Liaoning Natural Fund Guidance Plan (Grant No. 2019-ZD-0446 and Grant No. 201602701) is gratefully acknowledged.

References

[1] S.J. Leevers, B. Vanhaesebroeck, M.D. Waterfield, Signalling through phosphoinositide 3-kinases: the lipids take centre stage, Curr. Opin. Cell Biol. 11 (1999) 219–225.
[2] P. Liu, H. Cheng, T.M. Roberts, J.J. Zhao, Targeting the phosphoinositide 3-kinase pathway in cancer, Nat. Rev. Drug Discovery 8 (2009) 627–644.
[3] A.E. Garces, M.J. Stocks, Class 1 PI3K clinical candidates and recent inhibitor design strategies: a medicinal chemistry perspective, J. Med. Chem. 62 (2018) 4815–4850.
[4] S.B. Prasad, S.S. Yadav, M. Das, A. Modi, S. Kumari, L.K. Pandey, S. Singh, S. Pradhan, G. Narayan, PI3K/AKT pathway-mediated regulation of p27Kip1 is associated with cell cycle arrest and apoptosis in cervical cancer, Cell. Oncol. 38 (2015) 215–225.
[5] M. Martini, M.C.D. Santis, L. Braccini, F. Gulluni, E. Hirsch, PI3K/AKT signaling pathway and cancer: an updated review, Ann. Med. 46 (2014) 372–383.
[6] J. Yang, J. Nie, X.L. Ma, Y.Q. Wei, Y. Peng, X.W. Wei, Targeting PI3K in cancer: mechanisms and advances in clinical trials, Mol. Cancer 18 (2019) 26.
[7] H.C. Tang, J.Y.C. Shen, B.M. Chan, Idelalisib (Zydelig), Pharmacol. Update 11 (2015) 5–10.
[8] A. Markham, Copanlisib: first global approval, Drugs 77 (2017) 2057–2062.
[9] H.A. Blair, Duvelisib: first global approval, Drugs 78 (2018) 1847–1853.
[10] L. Urquhart, FDA new drug approvals in Q2 2019, Nat. Rev. Drug Discovery 18 (2019) 575.
[11] K. Down, A. Amour, I.R. Baldwin, et al., Optimization of novel indazoles as highly potent and selective inhibitors of phosphoinositide 3-kinase δ for the treatment of respiratory disease, J. Med. Chem. 58 (2015) 7381–7399.
[12] H. Lee, K.H. Jung, Y. Jeong, S. Hong, S.S. Hong, HS-173, a novel phosphatidylinositol 3-kinase (PI3K) inhibitor, has anti-tumor activity through promoting apoptosis and inhibiting angiogenesis, Cancer Lett. 328 (2013) 152–159.
[13] O. Kim, Y. Jeong, H. Lee, S.S. Hong, S. Hong, Design and synthesis of imidazopyridine analogues as inhibitors of phosphoinositide 3-kinase signaling and angiogenesis, J. Med. Chem. 54 (2011) 2455–2466.
[14] H. Lee, S.J. Kim, K.H. Jung, M.K. Son, H.H. Yan, S. Hong, S.S. Hong, A novel imidazopyridine PI3K inhibitor with anticancer activity in non-small cell lung cancer cells, Oncol. Rep. 30 (2013) 863–869.
[15] Y.H. Fan, W. Li, D.D. Liu, M.X. Bai, H.R. Song, Y.N. Xu, S.K. Lee, Z.P. Zhou, J. Wang, H.W. Ding, Design, synthesis, and biological evaluation of novel 3-substituted imidazo[1,2-a]pyridine and quinazolin-4(3H)-one derivatives as PI3Kα inhibitors, Eur. J. Med. Chem. 139 (2017) 95–106.
[16] S.D. Knight, N.D. Adams, J.L. Burgess, A.M. Chaudhari, M.G. Darcy, C.A. Donatelli, J.I. Luengo, K.A. Newlander, C.A. Parrish, L.H. Ridgers, Discovery of GSK2126458, a highly potent inhibitor of PI3K and the mammalian target of rapamycin, ACS Med. Chem. Lett. 1 (2010) 39–43.
[17] X.Q. Lv, H.Z. Ying, X.D. Ma, N. Qiu, P. Wu, B. Yang, Y.Z. Hu, Design, synthesis and biological evaluation of novel 4-alkynyl-quinoline derivatives as PI3K/mTOR dual inhibitors, Eur. J. Med. Chem. 99 (2015) 36–50.
[18] J.S. Han, Y. Chen, C. Yang, T. Liu, M.P. Wang, H.J. Xu, L. Zhang, C.H. Zheng, Y.L. Song, Ju Zhu, Structure-based optimization leads to the discovery of NSC765844, a highly potent, less toxic and orally efficacious dual PI3K/mTOR inhibitor, Eur. J. Med. Chem. 122 (2016) 684–701.
[19] V. Asati, D.K. Mahapatra, S.K. Bharti, PI3K/Akt/mTOR and Ras/Raf/MEK/ERK signaling pathways inhibitors as anticancer agents: Structural and pharmacological perspectives, Eur. J. Med. Chem. 109 (2016) 314–341.
[20] J.D. Hughes, J. Blagg, D.A. Price, S. Bailey, G.A. DeCrescenzo, R.V. Devraj, E. Ellsworth, Y.M. Fobian, M.E. Gibbs, R.W. Gilles, Physiochemical drug properties associated with in vivo toxicological outcomes, Bioorg. Med. Chem. Lett. 18 (2008) 4872–4875.